Agricultural Water Management 255 (2021) 107003

Contents lists available at ScienceDirect

Agricultural Water Management

journal homepage: www.elsevier.com/locate/agwat

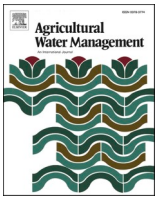

Optimization algorithms as training approaches for prediction of reference evapotranspiration using adaptive neuro fuzzy inference system

Dilip Kumar Roy [a,*], Alvin Lal [b], Khokan Kumer Sarker [c], Kowshik Kumar Saha [d], Bithin Datta [e]

[a] Irrigation and Water Management Division, Bangladesh Agricultural Research Institute, Gazipur 1701, Bangladesh
[b] Discipline of Civil Engineering, School of Information Technology, Engineering, Mathematics & Physics, University of the South Pacific, Fiji
[c] Soil and Water Management Section, Horticultural Research Center, Bangladesh Agricultural Research Institute, Gazipur 1701, Bangladesh
[d] Department of Agromechatronics, Technical University of Berlin, 10623 Berlin, Germany
[e] Discipline of Civil Engineering, College of Science and Engineering, James Cook University, QLD 4811, Australia

ARTICLE INFO

Handling Editor: J.E. Fernández

Keywords:
Reference evapotranspiration
Hybridized ANFIS models
Shannon's entropy
Grey relational analysis
Variation coefficient

ABSTRACT

Reference evapotranspiration (ET_0), widely used in efficient and meaningful scheduling of irrigation events, is an essential component of agricultural water management strategy for proper utilization of limited water resources. Accurate and early prediction of ET_0 can provide the basis for designing effective irrigation scheduling and help in resourceful management of water in agriculture. This study aims to evaluate and compare the performances of different hybridized Adaptive Neuro Fuzzy Inference System (ANFIS) models with optimization algorithms for predicting daily ET_0. The FAO-56 Penman-Monteith method was used to estimate daily ET_0 values using historical weather data obtained from a weather station in Bangladesh. The obtained climatic variables and the estimated ET_0 values form the input-output training patterns for the hybridized ANFIS models. The performances of these hybridized ANFIS models were compared with the classical ANFIS model tuned with combined Gradient Descent method and the Least Squares Estimate (GD-LSE) algorithm. Performance ranking of these ANFIS models was performed using Shannon's Entropy (SE), Variation Coefficient (VC), and Grey Relational Analysis (GRA) based decision theories supported by eight statistical indices. Results indicate that both SE and VC based decision theories provided the similar ranking though the numeric values of weights differed. On the other hand, GRA provided a slightly different sequence of ranking. Both SE and VC identified Firefly Algorithm-ANFIS (FA-ANFIS) as the best performing model followed by Particle Swarm Optimization-ANFIS. In contrast, FA-ANFIS was found to be the second-best performing model according to the ranking provided by GRA with a negligible difference in weight between FA-ANFIS and the classical ANFIS model (GD-LSE-ANFIS). Therefore, FA-ANFIS can be considered as the best model, which can be utilized to predict daily ET_0 values for areas with similar climatic conditions. The findings of this research is of great importance for the planning of effective irrigation scheduling.

1. Introduction

Changing weather patterns have been responsible for affecting agriculture to a great extent in recent years. As such, accurate and reliable prediction of weather variability have achieved a particular importance in agriculture related water resources planning and management problems. Reference evapotranspiration (ET_0) is the key parameter affecting efficient water management strategies in agriculture and is an important component in hydrological and ecological processes controlling agricultural water management. Accurate and early prediction of ET_0 provide the basis for designing efficient irrigation scheduling strategies in which actual crop evapotranspiration, ET_a can be obtained from the computed ET_0 when the crop coefficient values of the region of interest are known. Therefore, the applicability of ET_0 has gained wider popularity as it can be admirably adapted to various crops through the incorporation of crop coefficient values (Xiang et al., 2020). Accurate measurements of ET_0 can be obtained through lysimeters, which is generally used to develop and validate other indirect methods of ET_0 estimation (Allen et al., 2011; López-Urrea et al., 2006). These indirect methods are typically mathematical models that employ few meteorological information (e.g., air temperatures, relative humidity, solar radiation, and wind speed) obtained from meteorological stations of interest for estimating ET_0. As direct measurements through lysimeters and other approaches are cost intensive, indirect measurements

* Corresponding author.
E-mail address: dilip.roy@my.jcu.edu.au (D.K. Roy).

https://doi.org/10.1016/j.agwat.2021.107003
Received 17 October 2020; Received in revised form 13 May 2021; Accepted 29 May 2021
Available online 8 June 2021

have gained considerable attention in recent years.

Several empirical methods have been proposed by the United Nation's Food and Agriculture Organization (FAO) to estimate ET_0 values. Among them, the FAO-56 Penman-Monteith (FAO-56 PM) method (Allen et al., 1998) received considerable attentions in recent years and is considered as the standard method for the definition and estimation of ET_0 (Allen et al., 1998) as this method can be applied in a wide range of environments and climatic conditions without needing local calibrations due to its physical basis. The FAO-56 PM is a well-documented method that has been tested and validated for a huge bunch of meteorological settings covering a wide range of geographic locations (Landeras et al., 2008). However, given that this method requires a considerable amount of reliable and high-quality meteorological data for accurate estimation of ET_0, its use has become a major challenge particularly in developing countries where getting reliable data could often be a major hindrance. To minimize this drawback of data scarcity, Artificial Intelligence (AI) based models have been employed in predicting ET_0 values in several recent studies (Ahmadi et al., 2021; Chia et al., 2021; Elbeltagi et al., 2020; Feng et al., 2017c, 2017a; Granata, 2019; Roy et al., 2020; Tao et al., 2018; Yan et al., 2021; Wang et al., 2019; Wu et al., 2019). Nevertheless, the implementation of AI models requires an adequate number of input-output training patterns obtained either from direct measurements or indirect estimation of ET_0 from meteorological variables. It is noted that, AI based modelling approaches do not incorporate underlying physical processes of a system in predicting ET_0. However, once trained properly without model over- or under-fitting, AI based modelling approaches can provide reasonably accurate estimates of future ET_0 values when they are trained with the available input-output training patterns of meteorological variables and computed ET_0 values. The trained and validated models can provide hundreds even thousands of future ET_0 estimates without the need for calculating point ET_0 values for a particular set of input variables. In other words, once a relationship between the climatic variables and ET_0 can be established, one can obtain future values of ET_0 from that relationship rather than computing ET_0 values from the climatic variables using the FAO-56 PM equation. Nevertheless, the basis for developing this input-output relationship is entirely based on ET_0 computations using the FAO-56 PM method.

Numerous AI based models have been employed in recent years to accurately predict ET_0 values with meteorological variables as inputs to the AI models and calculated ET_0 values as outputs from the AI models. For instance, Feng et al. (2017a) evaluated the performances of Random Forests (RF) and Generalized Regression Neural Networks (GRNN) to estimate daily ET_0 values in southwest China. Their results indicated that both RF and GRNN models provided acceptable estimates of ET_0 and that prediction accuracy of RF was slightly better than that of the GRNN model. In another study, the performance of Extreme Learning Machine (ELM) and GRNN was found to be satisfactory in estimating daily ET_0 using only the temperature data in six meteorological stations in Sichuan basin of southwest China (Feng et al., 2017c). They concluded that both GRNN and ELM models outperformed temperature-based Hargreaves model and its calibrated version. Goyal et al. (2014) investigated the capabilities of Artificial Neural Networks (ANN), Least Squares – Support Vector Regression (LS-SVR), Fuzzy Logic, and Adaptive Neuro-Fuzzy Inference System (ANFIS) based AI models to enhance the accuracy of daily pan evaporation estimation in sub-tropical climates of Karso watershed in India. They concluded that Fuzzy Logic and LS-SVR based models provided the better prediction results when compared with ANN and ANFIS based models and that the AI based models outperformed the empirical Hargreaves and Samani as well as the Stephens–Stewart method. Ferreira et al. (2019) evaluated the performances of ANN and SVM based AI models for estimating ET_0 across Brazil using measured data on temperature and relative humidity or only temperature. Sanikhani et al. (2018) conducted a survey of different data-intelligent modelling strategies for air temperature forecasting. Yu et al. (2020) performed uncertainty analysis of AI-based modeling approaches for daily ET_0 prediction in the northwest end of China.

On top of the standalone AI based models, hybridized AI models have received a considerable attention, primarily to enhance the performance of standalone AI models in predicting ET_0 values. For instance, Tao et al. (2018) compared prediction accuracies of a Firefly Algorithm (FA) tuned ANFIS (FA-ANFIS) with the classical ANFIS model and concluded that FA-ANFIS provided better accuracy than the classical ANFIS model. Similarly, Wu et al. (2019) provided a comparison of four Extreme Learning Machine (ELM) based models optimized with bio-inspired optimization algorithms in predicting daily ET_0 and observed that ELM optimized with Flower Pollination Algorithm and ELM with Cuckoo Search Algorithm had better prediction accuracies when compared to the classical ELM model. Swarm based optimization algorithms, i.e., Particle Swarm Optimization (PSO), Moth-Flame Optimization (MFO), and Whale Optimization Algorithm (WOA) were also employed to develop hybrid ELM models (Chia et al., 2021) for ET_0 prediction. Their results revealed the superiority of WOA in developing hybridized ELM models. Wu et al. (2021) proposed a Kernel ELM (KELM) model hybridized with K-means clustering and FA (FA-KELM) to estimate ET_0. Their findings revealed that the FA-KELM model had slightly better performance when compared to the performances of ANFIS and that both FA-KELM and ANFIS produced superior performances to RF and M5 prime model tree. In another study, Ahmadi et al. (2021) proposed a hybrid SVR model optimized with Intelligent Water Drops (IWA) algorithm for estimating monthly ET_0 time series and concluded that the hybrid SVR model outperformed the standalone SVR model. Mohammadi and Mehdizadeh (2020) investigated the performance of WOA tuned SVR model and concluded that the hybrid SVR model outperformed the classical standalone SVR model in predicting daily ET_0 values. Extreme Gradient Boosting (XGB) model was hybridized with WOA (XGB-WOA) to estimate daily ET_0 values (Yan et al., 2021) in a humid region of China. Their findings indicated that the XGB-WOA model trained with external data and tested with local data provided reliable daily ET_0 estimates. They also observed that when synthetic data from the target and adjacent stations were used, external XGB-WOA model produced an ET_0 estimate that was better than or comparable to local XGB-WOA models.

Recent literature of AI based ET_0 modelling revealed that neural architectures have attained significant prediction accuracies for ET_0 modelling (Kumar et al., 2011). A neural architecture integrated with the concept of fuzzy logic theory, known as an ANFIS, has received considerable attention in recent years due to its better prediction capabilities over other AI based ET_0 models (Citakoglu et al., 2014; Cobaner, 2011; Fatemeh et al., 2012; Kisi et al., 2015; Ladlani et al., 2014; Patil and Deka, 2017). ANFIS models are benefited by the advantageous features of fuzzy logic theory and the adaptive nature of neural network architectures in solving nonlinear problems having a considerable amount of uncertainty (Jang, 1993). Fuzzy logic concept enables an ANFIS model to incorporate fuzziness, imprecision, and vagueness of the prediction dataset. Nevertheless, ANFIS models are associated with the limitations related to difficulties in optimizing internal parameters. Classical ANFIS models use a hybrid tuning algorithm based on gradient descent and least squares which are prone to be trapped in local optima (Peyghami and Khanduzi, 2013). This is particularly true when the network structure and adjustable model parameters are large in which case the classic ANFIS models might fail to tune the parameters perfectly and consequently the training of ANFIS models might not be satisfactory. Satisfactory training of an ANFIS model depends on the efficiency and accuracy of the training algorithm used (Hassanvand et al., 2018). Nature-inspired evolutionary algorithms have overcome the issues of slow and premature convergence in local optima, and therefore, have been a better choice to tune ANFIS model parameters for ET_0 modelling (Azad et al., 2019; Tao et al., 2018). Although a few evolutionary algorithms, e.g. Ant Colony Optimization for the continuous domain (ACOR), Genetic Algorithm (GA), Differential Evolution (DE), Firefly Algorithm (FA) and Particle Swarm Optimization (PSO) have been utilized recently to tune ANFIS parameters for ET_0

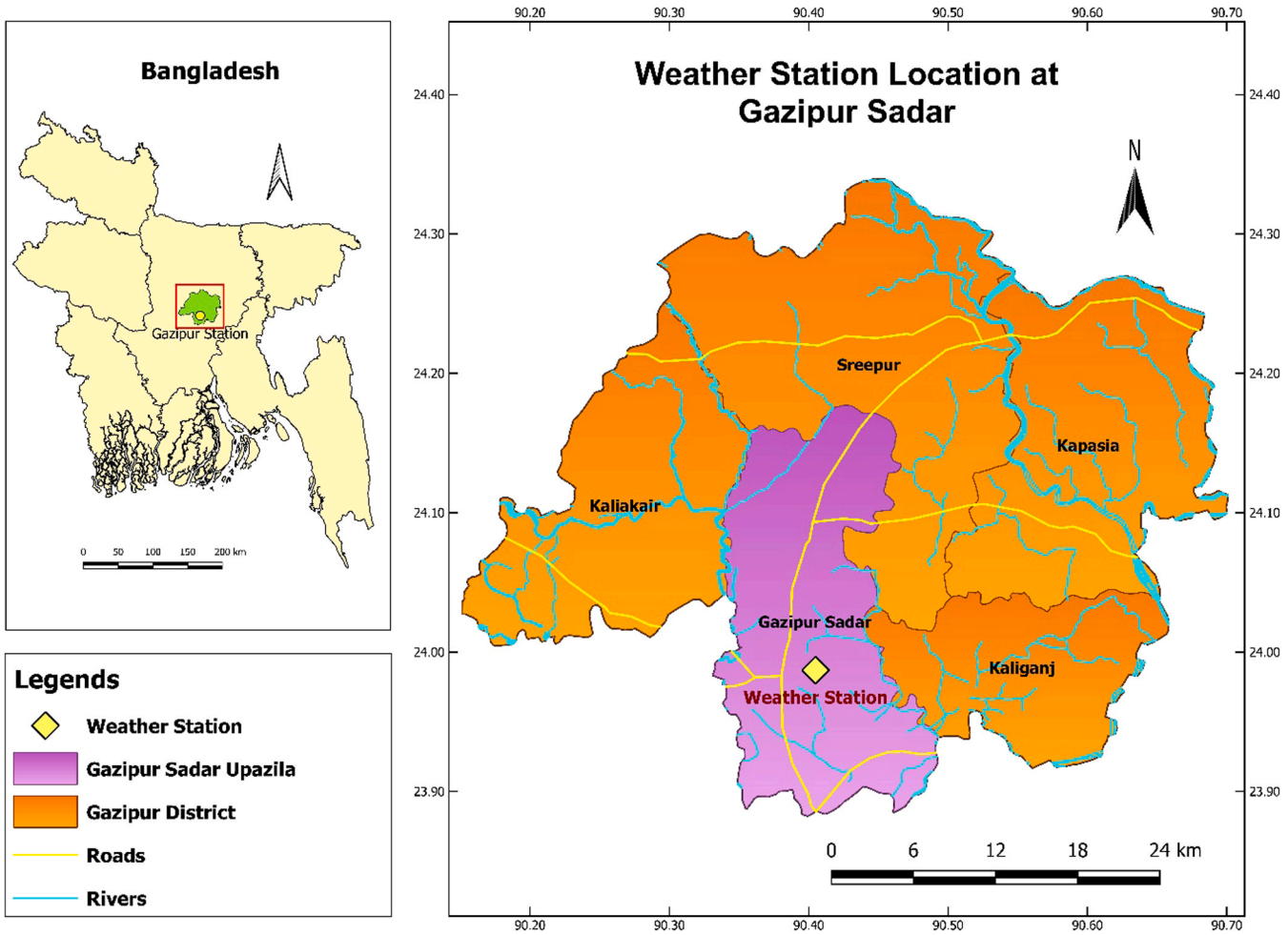

Fig. 1. Location of weather station in the study area.

modelling, a detailed comparison of several algorithms might be useful to obtain the best hybrid ANFIS model. Therefore, present study intends to provide a comprehensive comparison of several optimization algorithm tuned ANFIS models in developing daily ET_0 modelling.

While AI-based prediction models are effective tools in forecasting daily ET_0 values, accuracy and reliability of prediction largely depend on right choice of models for a particular study area. A set of performance evaluation indices are usually used to decide on the best performing model from a set of different models. However, the prediction models might have conflicting characteristics with respect to various performance indices. For instance, one prediction model might perform better than others with respect to correlation coefficient viewpoint, whereas another prediction model might have better performance when relative error criterion is used. To avoid this conflict, a set of performance indices should be incorporated in the decision-making process to address this contradiction objectively. In this approach, the performance indices are divided into benefit indices (the higher the better) and cost indices (the smaller the better). This study used four benefit and four cost indices in the decision-making process to rank the prediction models in terms of accuracy of prediction. The decision making was performed by calculating the weights of each hybridized model using these indices and with the aid of the concepts of Shannon's Entropy (SE) (Shannon, 1948), Variation Coefficient (VC) (Zhang and Xie, 2010), and Grey Relational Analysis (GRA) (Deng, 1982). Ranking of the prediction models was objectively performed by assigning these weights to each of these performance evaluation indices.

The concepts of information entropy or SE rely on the principle that the quantity and quality of information gained from the decision-making process determines the reliability and accuracy of the decision making (Wu et al., 2011). Entropy is a powerful tool for obtaining valuable information from the data and to quantify the amount of information contained in the data. The concept of entropy has been successfully applied in different research domains in recent years (Wang et al., 2015; Zhang et al., 2010). Likewise, the VC method is a typical diversity-based weighting method that calculates attribute weight resulting from the diversity or dipartite extent of attribute data among the feasible alternatives (Li et al., 2019; Liu et al., 2018; Xu et al., 2018) thus avoiding the deviance of human influences effectively (Ding et al., 2016). The VC approach computes weights using the attribute's coefficient of variation, which measures the extent of diversity of attributes (Chen, 2019). This weighting method has been used in the risk assessment and decision making regarding natural hazards (Chen, 2019; Li et al., 2019; Liu et al., 2018). On the other hand, GRA is an important part of Gray system theory (Deng, 1982) and can be applied to solve multi-criteria decision-making problems by integrating the whole range of performance index values considered for each alternative into an enumerated value of Gray relational grade. GRA has been successfully applied in various research niches, i.e., in deriving optimal operating rules for a hydropower reservoir (Fang et al., 2018), in an integrated cascade utilization system of geothermal water (Luo et al., 2016), and in the assessment of mine safety (Xu and Xu, 2018) etc. However, the application of these weighting approaches is quite limited in the ranking of evolutionary algorithm tuned ANFIS models for ET_0 prediction. To the best of the authors knowledge, the application of SE, VC, and GRA approaches has only been utilized in few recent studies for prioritizing the prediction models to develop ET_0 prediction modelling (Roy et al., 2020).

This study proposed 15 evolutionary algorithms, i.e., Artificial Bee Colony (ABC), Bee Algorithm (BA), Biogeography-based Optimization (BBO), Continuous Ant Colony Optimization (ACOR), Covariance Matrix Adaptation Evolution Strategy (CMA-ES), Cultural Algorithm (CA), Differential Evolution (DE), Firefly Algorithm (FA), Genetic Algorithm (GA), Harmony Search (HS), Imperialist Competitive Algorithm (ICA), Invasive Weed Optimization (IWO), Particle Swarm Optimization (PSO), Simulated Annealing (SA) and Teaching-Learning-based Optimization (TLBO) to develop hybridized ANFIS models for ET_0 forecasting. The performances of these hybridized ANFIS models were compared with those of the classic ANFIS model. Finally, a ranking of the performances of developed hybridized ANFIS models was proposed using the concepts of three decision theories (SE, VC, and GRA). The methodology was demonstrated using a case study in a sub-tropical climate in Bangladesh. Therefore, the prime focus of this research work is to improve the ANFIS performances using several optimization algorithms. Another contribution of this work is the selection of best ANFIS model utilizing decision theories that incorporate eight statistical performance evaluation indices instead of relying on few performance indices in reaching the conclusion. Therefore, the study not only proposes several optimization algorithms for better ANFIS tuning but also provides a decision tool through which one can select the best ANFIS model for ET_0 prediction.

To the best of the authors understanding, there has been a lack of comprehensive comparison of several optimization algorithms in improving the ANFIS performance for daily ET_0 estimation. Besides, there has been a need to provide a ranking of the performances of optimization algorithm tuned ANFIS models using several performance indices instead of relying on few indices. The main contribution of this study is to select a suitable optimization algorithm tuned ANFIS model utilizing three decision theories for daily ET_0 prediction. While successful tuning of ANFIS parameters through optimization algorithms can improve prediction accuracy, incorporation of decision theories will assist decision makers in taking right decision to select the best prediction model. As it is practically infeasible to attempt all available optimization algorithms, the scope of the present study has been limited to few of the promising algorithms to be integrated with the ANFIS. Hence, the aim of this study is to (1) employ 15 optimization algorithms to tune ANFIS parameters; (2) provide a comparison of the performances of hybridized ANFIS models; and (3) provide a ranking of the hybridized ANFIS models utilizing three decision theories. The findings of this study will be of crucial importance to the agricultural especially irrigation perspective as an alternative modelling approach and, in particular, within the context of developing countries like Bangladesh where monitoring and acquisition of reliable meteorological data is a serious concern.

2. Methodology

2.1. Study area and data

The historical daily weather data were obtained from an automatic weather station located in Gazipur Sadar Upazilla (located at 24.00° north latitude and 90.43° east longitude) of Gazipur district in Bangladesh. The study area covers an aerial extent of approximately 446.38 km^2. The average annual rainfall of the study area is 2036 mm of which around 80% occurs during the months of May to August (monsoon season in Bangladesh). Generally, the study area is in a sub-tropical climatic zone with heavier rainfalls in the summer and lighter rainfalls in winter. The weather station is situated at 24.00° north latitude and 90.41° east longitude with an elevation of 8.4 m above mean sea level. The location of the weather station is illustrated in Fig. 1. The climatic variables such as minimum and maximum air temperatures, relative humidity, wind speed, and sunshine duration for a period of approximately 15 years (01 January 2004–30 June 2019) were obtained from the weather station shown in Fig. 1. The amount of sunshine as well as length of the day was obtained from a silicon photo diode type global solar radiation recorder (Licor-200SZ, LI-COR Biosciences, USA; accuracy = ± 5%; range = 0.3–4 μm; measurement height = 2 m). The maximum and minimum thermometers (Zeal P1000, G. H. Zeal Ltd., UK; accuracy = ± 0.2℃; range and resolution = − 50 to + 70 ℃, 0.1 ℃; measurement height = 2 m) were used to measure the maximum and minimum temperatures of the day, respectively. A capacitive type hygrometer (R. M. Young Company, USA; accuracy = ± 3%; range and resolution = 0–100%, 1%; measurement height = 2 m) was used to measure relative humidity. A rotating cup anemometer (Cup Anemometer 4.3018.10.000, Adolf Thies GmbH & Co. KG, Germany; accuracy = 1.2 m/s; range and resolution = 0.5–60 m/s, 0.1 m/s; measurement height = 10 m) was used to measure the wind speed. It is noted that few adjustments were needed to get to the FAO-56 PM method suitable for local conditions as well as to improve the ET_0 estimations (Allen et al., 2006). For instance, the obtained wind speed at 10 m height was converted to a height of 2 m, keeping a lower limit of 0.5 m/s following the recommendations from Allen et al. (2006).

Table 1
Statistics of the obtained meteorological variables.

Variables	Min	Max	Mean	Standard deviation	Skewness	Kurtosis
Minimum temperature, °C	4.40	34.50	21.17	5.64	-0.63	-0.88
Maximum temperature, °C	12.00	53.00	30.93	3.92	-1.10	2.11
Relative humidity, %	38.00	89.00	80.22	8.20	-0.63	0.75
Wind speed, m/s	0.68	5.06	2.79	1.05	-0.06	-1.32
Sunshine duration, h	0.00	11.40	5.54	3.09	-0.40	-1.04

The descriptive statistics of the obtained meteorological variables is presented in Table 1.

The ET_0 values were calculated using the weather data inputted into the FAO-56 PM model (Allen et al., 1998). Net radiation at the crop surface (calculated from the obtained sunshine hours) and other four climatic variables were used to calculate the ET_0. This method is commonly accepted by scientific communities, and has become an extensively used approach in situations where the ET_0 values are difficult to acquire experimentally (Allen et al., 1998; Feng et al., 2017b; Shiri et al., 2014). The FAO-56 PM model can be represented by:

$$ET_0 = \frac{0.408\Delta(R_n - G) + \gamma \frac{900}{T_{mean}+273} u_2 (e_s - e_a)}{\Delta + \gamma(1 + 0.34u_2)} \quad (1)$$

where, ET_0 is the reference evapotranspiration, mm/d; R_n is the net radiation at the crop surface, $MJ/m^2/d$; G is the heat flux density of soil, $MJ/m^2/d$; Δ is the slope of the saturation vapor pressure curve, kPa/°C; γ is the psychometric constant, kPa/°C; e_s is saturation vapor pressure, kPa; e_a is actual vapor pressure, kPa; u_2 is the wind speed at a height of 2 m, m/s; and T_{mean} is mean air temperature at 2 m height, °C.

The mean saturation vapour pressure (e_s) is derived from air temperature. The relationship between air temperature and $e_{(T)}$ can be represented by the following equation (Zotarelli et al., 2010):

$$e_{(T)} = 0.6108 exp\left[\frac{17.27T}{T + 237.3}\right] \quad (2)$$

where, $e_{(T)}$ = Saturation vapour pressure at the air temperature T, kP_a; and T = air temperature, ℃.

As such, e_s is computed as the average values between the saturation vapour pressure at both the maximum and minimum values of daily air temperature such that,

$$e_{(T_{max})} = 0.6108 exp\left[\frac{17.27T_{max}}{T_{max} + 237.3}\right] \quad (3)$$

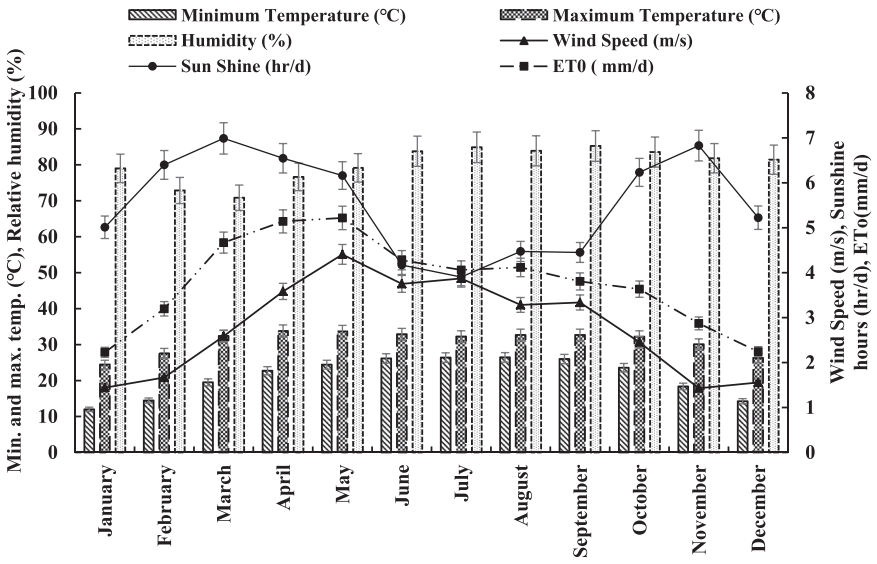

Fig. 2. Monthly average of climatic variables and calculated ET_0 values. The primary axis displays Temperature (minimum and maximum temperature, ℃), and Relative humidity (%) whereas the secondary axis depicts Wind Speed (m/s), Sunshine hours (hr/d), and ET_0 (mm/d).

$$e_{(T_{min})} = 0.6108 exp\left[\frac{17.27 T_{min}}{T_{min} + 237.3}\right] \tag{4}$$

where, T_{max} = daily maximum air temperature, ℃; and T_{min} = daily minimum air temperature, ℃. The e_s thus be calculated using the following equation:

$$e_s = \frac{e_{(T_{max})} + e_{(T_{min})}}{2} \tag{5}$$

On the other hand, actual vapour pressure (e_a) is computed from the relative humidity:

$$e_a = \frac{e_{(T_{min})}\left[\frac{RH_{max}}{100}\right] + e_{(T_{max})}\left[\frac{RH_{min}}{100}\right]}{2} \tag{6}$$

where, e_a = actual vapour pressure, kP_a; $e_{(T_{min})}$ = saturation vapour pressure at minimum daily temperature, kP_a; $e_{(T_{max})}$ = saturation vapour pressure at maximum daily temperature, kP_a; RH_{max} = maximum relative humidity, %; and RH_{min} = minimum relative humidity, %.

Slope of the saturation vapor pressure curve (Δ) and psychrometric constant (γ) are calculated as (Allen et al., 1998):

$$\Delta = \frac{4098\left[0.6108 \quad exp\left(\frac{17.27T}{T+237.3}\right)\right]}{(T + 237.3)^2} \tag{7}$$

$$\gamma = \frac{C_p P}{\varepsilon\lambda} 0.665 \times 10^{-3} P \tag{8}$$

$$P = 101.3\left(\frac{293 - 0.0065Z}{293}\right)^{5.26} \tag{9}$$

where, exp [•] is 2.7183 (base of the natural logarithm) raised to the power [••]; P represents the atmospheric pressure, kPa; λ denotes the latent heat of vaporization (2.45 MJ/kg); C_p is the specific heat at constant pressure (1.013×10^{-3}MJ/kg/℃); ε is the ratio between molecular weight of water vapor and dry air (*molecular weight of water vapour/dry air*) (0.622).

The net radiation (R_n) is calculated as:

$$R_n = R_{ns} - R_{nl} \tag{10}$$

where, R_{ns} = incoming net shortwave radiation, MJ/m^2/d; R_{nl} = outgoing net longwave radiation, MJ/m^2/d.

The net shortwave radiation (R_{ns}) can be computed from the following equation:

$$R_{ns} = (1 - a)R_s \tag{11}$$

where, a = canopy reflection coefficient or albedo (dimensionless), the value of which is 0.23 for the hypothetical grass reference crop, and R_s = incoming solar radiation, MJ/m^2/d.

$$R_s = \left[a_s + b_s\frac{n}{N}\right]R_a \tag{12}$$

where, R_a is the extra-terrestrial radiation, MJ/m^2/d; N and n are, respectively, the maximum and actual possible sunshine durations. The recommended values for a_s and b_s are 0.25 and 0.50, respectively (Allen et al., 1998).

$$R_a = \frac{24(60)}{\pi} G_{sc} d_r[\omega_s sin(\varphi) sin(\delta) + cos(\varphi) cos(\delta) sin(\omega_s)] \tag{13}$$

where, G_{sc} is the solar constant (0.0820 MJ/m^2/min; d_r is the inverse relative distance Earth-Sun; ω_s represents the sunset hour angle, rad, φ indicates latitude, rad, and δ is the solar declination.

$$d_r = 10.033 \quad cos\left(\frac{2\pi}{365} J\right) \tag{14}$$

where, J represents the number of days in a year between 1 (January 1) and 365 or 366 (December 31).

$$\delta = 0.409 \quad sin\left(\frac{2\pi}{365} J - 1.39\right) \tag{15}$$

$$\omega_s = arccos[-tan\varphi tan\delta] \tag{16}$$

$$Radians = \pi/180(decimal\ degrees) \tag{17}$$

The net outgoing longwave radiation (R_{nl}) is represented by:

$$R_{nl} = \sigma\left[\frac{(T_{max} + 273.16)^4 + (T_{min} + 273.16)^4}{2}\right](0.34 - 0.14)\sqrt{e_a}\left[1.35\frac{R_s}{R_{so}} - 0.35\right] \tag{18}$$

R_{so} in Eq. (18) is calculated using the following equation:

$$R_{so} = \left(0.75 + 2 \times 10^{-5} Z\right) R_a \quad (19)$$

u_2 in Eq. (1) is calculated using the following equation (Allen et al., 1998):

$$u_2 = u_z \frac{4.87}{ln(67.8z - 5.42)} \quad (20)$$

where, T_{max} and $T_{min} = K$ maximum and minimum absolute temperatures during the 24-hour period [$K = ℃ + 273.16$]; R_{so} = clear sky solar radiation, MJ/m^2/d, σ represents the Stefan-Boltzmann constant (4.903×10^{-9} MJ/K^4/m^2/d); u_z is the measured wind speed at Z_m above the ground surface, m/s; z represents the elevation of the station above the mean sea level, m. Estimated ET_0 values ranged from 0.92 mm/d to 8.02 mm/d while the mean, standard deviation, skewness, and kurtosis values were 3.80 mm/d, 1.32 mm/d, 0.30, and − 0.67, respectively. Fig. 2. shows average values of the climatic variables and calculated ET_0.

These calculated ET_0 values and the climatic variables were used as outputs and inputs, respectively, of the developed ANFIS based models. The entire input-output datasets were divided into training (80%), validation (10%), and test sets (10%). The dataset contains 5660 entries of climatological variables and computed ET_0 values. The first 4528 entries (from 01 January 2004–24 May 2016) counting 80% of the total data were used as training patterns whereas the next 566 entries counting 10% of the total data (from 25 May 2016–11 December 2017) were used as validation dataset to validate the developed ANFIS models. It is noted that the training and validation were performed simultaneously. The remaining 10% (566 entries, i.e., from 12 December 2017–30 June 2019) of the total dataset was used as test dataset to test the trained and validated ANFIS models. As there remains no definite rules for data partitioning, this partitioning scheme of 80-10-10 was selected after conducting several trials (results are not presented).

2.2. Adaptive Neuro-fuzzy Inference System (ANFIS)

ANFIS models are able to mimic the trends of the input-output patterns of a nonlinear system due to their capability of incorporating vagueness or fuzziness of the input parameters of a complex system (Jang et al., 1997). For this reason, ANFIS models are often considered to be the universal approximators of nonlinear and complex systems. Incorporation of advantageous features of both the fuzzy logic and artificial neural networks has made them capable of modelling nonlinear processes of complex systems through capturing and mapping the trends or relationships between the input and output variables (Sugeno and Yasukawa, 1993; Takagi and Sugeno, 1985). A Sugeno type ANFIS model has a relatively simple architecture with the ability of providing a fairly accurate prediction through superior learning capability (Jang et al., 1997). In this effort, Fuzzy C-Mean Clustering (FCM) (Bezdek et al., 1984) algorithm was utilized to reduce the dimensionality of the training dataset in order to minimize the numbers of modifiable (linear and nonlinear) parameters of the developed ANFIS models. The input and output membership functions of a Sugeno type ANFIS are Gaussian and linear, respectively. The Gaussian membership function, determined by two parameters $\{c, \sigma\}$, can be represented by (after Jang et al. (1997)):

$$gaussian\ (x, c, \sigma) = e^{-\frac{1}{2}\left(\frac{x-c}{\sigma}\right)^2} \quad (21)$$

where, c = center of the membership function, and σ = width of the membership function. Fig. 3 illustrates an ANFIS architecture derived from a Sugeno type Fuzzy Inference System (FIS).

The building block of the ANFIS structure shown in Fig. 3 is the first-order Sugeno FIS, which is composed of two inputs (αandβ) and one output (f). The fuzzy if-then rule sets for this FIS can be written as:

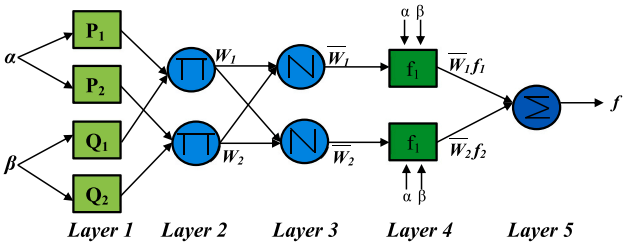

Fig. 3. ANFIS structure derived from a two-input first-order Sugeno type FIS (Jang, 1993).

$$Rule\ \ 1: If\ \alpha\ is\ P_1\ and\ \beta\ is\ Q_1\ then\ f_1 = p_1\alpha + q_1\beta + r_1 \quad (22)$$

$$Rule\ \ 2: If\ \alpha\ is\ P_2\ and\ \beta\ is\ Q_2\ then\ f_2 = p_2\alpha + q_2\beta + r_2 \quad (23)$$

The Sugeno type ANFIS has five layers as shown in Fig. 3. These layers are named as a fuzzy layer, a product layer, a normalized layer, a defuzzification layer, and a total output layer. The detail description and the functions of these layers can be found in Jang (1993) and is not repeated here.

MATLAB commands and functions were used to develop the ANFIS models.

2.3. Optimization algorithms for tuning ANFIS parameters

2.3.1. Artificial Bee Colony (ABC)

The ABC (Karaboga, 2005) is a relatively new swarm intelligence based meta-heuristic optimization algorithm that intends to simulate intelligent natural behavior of real honey bees in food forging. A swarm consists of a set of honeybees, which are assigned to perform particular tasks successfully accomplished through social cooperation. Honeybees utilize a number of unique mechanisms, for instance, waggle dance to accurately locate food sources and to search for new locations of food sources. This unique behavior of honeybees makes them an ideal candidate for formulating intelligent search algorithms. The ABC algorithm makes use of the performances of three types of bees (employed bees, onlooker bees and scout bees) associated with three types of actions: (i) search for new food sources, (ii) recruit bees for collecting the food, and (iii) abandon the exploited food sources. The employed bees search for food around the food source and transmit the information on the food sources to the onlooker bees who wait in the hive for the information from the employed bees. Scout bees are associated with searching for the new food sources. The employed bees dance in the dance area to transmit information about food sources and the dancing extent is proportional to the nectar content of the food sources exploited by the dancing bees a few moments ago. Onlooker bees select a food source by judging the quality of the food source perceived through the nature of dancing by the employed bees. When honeybees, be it an onlooker or a scout bee, find a food source they become employed bees. A food source is abandoned whenever it is fully exploited by the employed bees who may afterwards become onlooker or scout bees. In the ABC algorithm, the first and second halves of the swarm are composed of employed and onlooker bees, respectively. The number of solutions is equal to the number of either the employed or the onlooker bees in the swarm (Karaboga, 2005). The position of a food source represents a feasible solution of the optimization problem in hand whereas the nectar quantity of a food source represents the quality (fitness) of that solution. The details of the ABC algorithm with the associated equations can be found in Karaboga (2005), and are not repeated here.

2.3.2. Bee Algorithm (BA)

The BA, proposed by Pham et al. (2006), is similar to the ABC with respect to both local and global search processes. However, the algorithms differ in terms of neighborhood search process during which ABC

$i = 0$
Generate initial population of size$n$
Evaluate the Fitness Value of initial population
Sort the initial population on the basis of fitness value
Perform a *while loop* until the user defined maximum number of iterations (MaxIter) is reached OR the differences in Fitness Values between any two consecutive iterations becomes less than or equal to the used defined Error criterion(*Error*)
The While loop
while i $\leq$ MaxIter OR $\text{Fitness}_i - \text{Fitness}_{i-1} \leq$ Error
a. $i = i + 1$
b. Select the elite and non-elite best patches for performing neighborhood search
c. Employ the forager bees in the elite patches and the non-elite best patches
d. Evaluate the Fitness Value of each patch;
e. Sort the results based on their fitness values;
f. Allocate the reminder of the bees to the non-best locations to perform global search;
g. Evaluate the Fitness Value of the non-best patches;
h. Sort the overall results on the basis of their Fitness Values;
i. Execute the algorithm until the termination criterion/criteria is/are met
End

employs probabilistic approach whereas BA employs fitness evaluation approach to drive the search process (Yuce et al., 2013). The BA utilizes exploitation and exploration strategies in order to perform both local and global searches, respectively. The basic operating principle of the BA is as follows: Let *i* be the number of iterations, then the pseudo-code of the basic BA can be written as:

In BA, each point within the solution space is regarded as a food source. When a honeybee finds a food source, its quality is evaluated by the bee through the fitness function. Scout bees are assigned to randomly select the fitness landscape with a priority of sampling unexplored areas of higher fitness. That is to say, new probable solutions are generated and evaluated randomly. The ranking of the visited areas is performed, and the forager bees are employed to re-search the neighborhood of the highly ranked locations, i.e., new solutions similar to the current best ones are generated and evaluated.

2.3.3. Biogeography-based Optimization (BBO)

The BBO (Simon, 2008) is developed by incorporating the ideas from biogeographic evolution. This evolutionary algorithm is intended to perform global optimization. In BBO, a population of habitats, referred to as solutions, are repeatedly evolved and improved principally by migrating characteristics from better solutions to worse ones. Each standalone solution, known as "habitat" or "island", has a particular Habitat Suitability Index (HSI). Emigration and immigration rates are computed using this HSI, which is used to determine the extent of suitability of solutions. A particular solution is considered to be more suitable if its HSI value is higher whereas a solution with a lower HSI value indicates a less suitable solution. Solutions with higher and lower HSI values have a tendency to share few of their unique features with each other (Zheng et al., 2014). Two major mechanisms namely migration and mutation control the continuous evolution and improvement of the habitats or solutions in BBO. BBO has proved itself as one of the promising evolutionary algorithms when tested with various test problems (Du et al., 2009; Simon, 2008; Song et al., 2010). A detailed description of the BBO can be found in Simon (2008), and is not repeated here.

2.3.4. Continuous Ant Colony Optimization (ACOR)

The first Ant Colony Optimization (ACO) was developed from an inspiration by the foraging behavior of real ants (Dorigo, 1992). During foraging, ants initially utilize a random search to explore the area surrounding their nest. Whenever an ant finds a source of food, it evaluates the source and brings some food to its nest. The ant deposits a pheromone trace on the path it uses to return to the nest. The amount of this deposited pheromone provides a signal to the other ants about the quantity and quality of the food. This pheromone track acts as an indirect form of communication among the ants enabling them to find the shortest routes between the food sources and the nest. Initial application of ACO was intended to solve Combinatorial Optimization Problems (COPs) including vehicle routing, scheduling, timetabling, and so on (Dorigo, 1992; Dorigo et al., 1999, 1996). Although a lot of real-world optimization problems can be represented as COPs directly, many of the real-world problems, for instance, those requiring selection of values for continuous variables may not be well suited to be represented as COPs directly. Such problems require converting the continuous ranges of allowable values into finite sets. However, this conversion is not always straightforward and expedient in cases where the initial probable range is extensive, and the process demands a very high resolution (Socha and Dorigo, 2008). To overcome this inconvenience associated with the original ACO algorithm, Socha and Dorigo (2008) proposed an extension of ACO algorithm to continuous domains without carrying out any major conceptual modification to the structure of the original ACO algorithm. This modified algorithm is referred to as ACOR.

According to Socha and Dorigo (2008), the formal definition of a model for continuous optimization problem can be expressed as:

$$Q = (\mathbf{S}, \Omega, f) \tag{24}$$

This model for continuous optimization problem includes:

a. a search space ($\mathbf{S}$) that is defined over a finite set of continuous variables
b. a set (Ω) of constraints among the variables
c. an objective function to be minimized that can be defined as: f:$\mathbf{S} \rightarrow \mathbb{R}_{+}^{0}$

The key idea associated with the ACOR algorithm is the shift from 'using a discrete probability distribution' to 'using a continuous probability distribution', commonly referred to as a probability density function. The ACOR consists of three major algorithmic components, namely, (i) Ant Based Solution Construction, (ii), Pheromone Update, and (iii) Daemon Actions. A detailed description of these components can be found in Socha and Dorigo (2008), and is not repeated here.

2.3.5. Covariance Matrix Adaptation Evolution Strategy (CMAES)

The CMAES is an efficient derivative-free global evolutionary optimization algorithm for solving continuous optimization problems (Hansen et al., 2003). It possesses several advantageous features, for instance, the CMAES is a derivative free, covariant, off-the-shelf, and

scalable optimization algorithm (Hansen et al., 2003). The CMAES is intended to optimize a black-box objective function over a well-defined parameter space (Dang et al., 2019). The feature functions are sometimes delineated manually within this parameter space. As such, the selected feature quality or the underlying parameter space largely influence the performance of this optimization approach (Dang et al., 2019). The working principle of CMAES is primarily governed by establishing a parametric distribution over the solution space. The algorithm utilizes a parametric search distribution for an iterative sampling of a population of candidate solutions, which are then evaluated by a black-box function (Dang et al., 2019). Like any other evolutionary optimization algorithm, the CMAES implements three key steps, namely recombination, mutation and selection in order to carry out the optimization tasks.

However, the original CMAES was slightly modified by Hansen et al. (2003) with a view to adapting the covariance matrix through utilizing additional information obtained from larger populations. In this modified version of the CMAES, higher rank information is included rather than using the rank one information for updating the covariance matrix. The modified equations can be found in Hansen et al. (2003), and is not repeated here.

2.3.6. Cultural Algorithm (CA)

The CA, proposed by Reynolds (1994), is a population-based optimization algorithm based on the concept of collective intelligence. It is derived from the '*lineal evolution of socio-cultural transition, which prevailed in the19th century*' (Kuo and Lin, 2013), and is employed as a search engine to solve global optimization problems. Reynolds (1994) described the fundamentals of CA using an expression of Renfrew's *Think* model with respect to a twofold inheritance framework. This framework incorporated a belief space that constitutes both the individual and group 'mappa', and a trait-based population space. In this framework, each of the individuals can be represented with respect to (a) a set of traits or behaviors, and (b) a 'mappa' or a general explanation of their understandings. Traits are possible to be altered and swapped between individuals with the help of various socially inspired operators whereas the individual 'mappa' may be combined and altered to create 'group mappa'. The symbols for characterizing traits and 'mappa' may also be altered with time with respect to the experience. Existing traits may be lost from the population while several new traits can be added to the population. Likewise, symbols representing 'mappa' may also be forgotten and new symbols may be added. Therefore, the depiction of the trait sequences and the 'mappa' may themselves be evolved with the utilization of the experiences of the groups.

At a certain time-step, there exists a set of individuals (each of which are defined with respect to the presently applicable traits) within the population space. Each individuals' performance is evaluated with respect to solving a given set of problems. Additionally, each individual is likely to create a general mapping of their experiences during this time-step, a process referred to as outlining. The most generalized belief in a created 'mappa' is named as its 'dominant belief'. The 'mappa' of an individual can then be combined with presently prevailing 'group mappa' within the belief space whenever the conditions for one or combining operations are satisfied. If a 'mappa' is unable to be merged for a certain time-step, it remains separated within the belief space for that time-step. During the merging of 'mappa', the performances of individuals allied with the 'mappa' are integrated. If the integrated performance of a 'mappa' is lower than some predefined level of acceptance, then that 'mappa' is eliminated or 'pruned' from the belief space. The set of presently accepted 'group mappa' forms the adjusted belief space for a particular time-step. Eliminated 'mappa' may or may not be enforced in the population level.

The present state of the belief space can, therefore, be utilized to alter the individuals' performance, alter the set of acceptable traits, and enforce eliminated 'mappa' etc. The population is then utilized to create a new population by means of the selection of individuals to be parents for the next generation. The parents are then employed to evolve a new population through the use of different alteration operators. A communication channel or protocol is employed to describe the effects of present belief space on the population of individuals as well as the counter effect of the individuals on the belief space. The vote-inherit-promote protocol is utilized. This protocol supports the method of connecting the performance of an individual with a 'mappa' in the belief space (vote), then letting the 'mappa' to inherit the performances of individuals (inherit), and eventually promoting those individuals in the population related to the present 'group mappa' (promote) (Reynolds, 1994). The process continues until a stopping or termination criterion is satisfied.

2.3.7. Differential Evolution (DE)

The DE algorithm (Price, 1999; Storn, 1999) is a stochastic and population-based optimization algorithm, ideally suited for solving nonlinear optimization problems. The concept of DE is simple with a fundamental configuration of DE/rand/1/bin (Fan and Lampinen, 2003; Storn and Price, 1997). In DE, an initial population is randomly generated following a uniform distribution with the lower and upper bounds of x_j^L and x_j^U, respectively. This randomly created initial population contains *NP* vectors such that $X_i, \forall_i = 1, 2, 3, \ldots, \mathrm{NP}$. Once this initialization process has completed, the generated individuals are evolved through mutation and crossover operators leading to the creation of a trial vector. The trial vector thus obtained is compared with the associated parent for selecting the vector that should pass through to the next generation (Das and Suganthan, 2011). The basic steps of DE algorithm are consisted of initialization, mutation, crossover, and selection. These steps are described in Price (1999) and in Storn (1999), and are not repeated here.

2.3.8. Firefly Algorithm (FA)

The development of FA (Yang, 2010) was inspired by the idealized behavior of the fireflies (light flashing characteristics). These light flashing characteristics of fireflies can be idealized into three basic rules:

a) Fireflies are unisex, and they possess a unique characteristic in order to attract each other regardless of the sex they belong to;
b) The rate of attraction is proportional to the degree of brightness. This implies that for any two fireflies with dissimilar flashing characteristics, the firefly possessing more brightness will attract the one with less brightness. In other words, the less bright firefly will tend to move towards the brighter firefly. Furthermore, both the brightness and attraction are inversely proportional to the distance, therefore, a firefly will move randomly if it cannot find no other brighter fireflies than itself;
c) The landscape of the objective function of a particular problem determines the brightness or light intensity of a firefly.

Thus, variation of light intensity and establishment of attraction are the two most important issues in the FA. In particular, it is perceived that the attraction of a firefly to another firefly is associated with the light intensity or brightness of the participating fireflies, and the light intensity is affected by the landscape of the encoded objective function. The details of FA can be found in Yang (2010) and are not repeated here.

2.3.9. Genetic Algorithm (GA)

GA was introduced by John Holland in 1960 and was further protracted by Goldberg (1989). GA works on the principles of natural selection method that initiates biological evolution based on Darwin's theory of evolution. It is capable of solving complex optimization problems with or without linear, nonlinear, and bound constraints. GA differs in principle from other classical optimization algorithms with respect to the coding of variables (GA employs coding of variable instead of the variables themselves) (Deb et al., 2002). GA is a population based

evolutionary algorithm that utilizes probability theorem in its search procedure for providing a population of solutions rather than generating a single solution. During the search process, a population of individual solutions is repetitively modified by the GA. At every step of the search process, the algorithm randomly chooses parents from the present population pool and employs these selected parents to generate children for the next generation. The population 'evolves' on the way to an ideal or optimal solution through an iterative process of the formation of a reasonable number of generations. To produce successive generations from the present population pool during each step, the GA employs three key categories of rules: selection, crossover, and mutation. Each of these rules is associated with performing particular tasks as the algorithm progresses to reach an optimal solution. These tasks are summarized as follows:

- Selection rules: They randomly select individuals or parents from the present pool of populations. These parents contribute in terms of producing offspring or children to the next pool of populations at successive generations.
- Crossover rules: These rules integrate two parents for producing offspring for the next generation.
- Mutation rules: They apply arbitrary alterations to individual parents to produce offspring.

The fundamental working principles of GA are summarized in the following points (Mathworks, 2020):

I. GA starts by forming a randomly generated initial population.
II. A sequence of new populations is then formed. During successive steps, GA employs individuals contained in the present generation to produce the next population. New population is produced through the subsequent phases:

- Scoring of all members of the present population through calculating their individual fitness values, which are referred to as 'raw fitness scores'.
- Converting the 'raw fitness scores' to a further usable array of values through scaling. These usable scaled values are named as 'expectation value'.
- Selecting parents with respect to their 'expectation values'.
- Selecting 'elite' members (having lower fitness values) from the present population and passing them to the next population.
- Producing offspring from the parents. Offspring production is performed either by mutation (a single parent is randomly changed) or by crossover (a pair of parents is combined).
- Replacing the present population with the produced offspring in order to create successive generations.

I. The iterations of GA search process terminate as soon as the user defined stopping criteria are satisfied.

2.3.10. Harmony Search (HS)

HS, a music-inspired metaheuristic optimization algorithm, was first proposed by Geem et al. (2001). The development of HS is stimulated by the fundamental ideologies of the musician's improvisation of the harmony (Gao et al., 2015). The algorithm is based on the observation that the prime objective of listening music is to look for an ideal situation of harmony, which is incorporated in the search process to obtain an optimal solution for an optimization problem. The link between the musical harmony and the optimal solution lies in the analogy between them in such a way that a musician constantly tries to present a piece of music with flawless harmony while an optimization problem formulation always intends to search for the best or optimal solution. Such linking or similarities motivated the researchers to develop HS algorithm through learning from both musical harmony and principles of optimization process. The HS is an attempt to transform the qualitative improvisation of a musician into several quantitative rules by idealization (Yang, 2009).

The idealization of an expert musician is associated with three probable selection processes. In the first case, a musician may decide to play any popular music with a sequence of harmonic pitches solely from his memory. Secondly, he may opt to play a recognized piece of music by modifying the existing harmonic pitch to some extent. Thirdly, the musician may choose to compose and play a completely new or random music. These three qualitative possibilities are incorporated into a quantitative optimization formulation in which these three components are accordingly named as: 'usage of harmony memory', 'pitch adjusting', and 'randomization' (Geem et al., 2001). The first component, 'usage of harmony memory', is very similar to the selection of best-fit individuals in GA and is an important constituent in HS algorithm. This component ensures the inclusion of the best harmonies to the successive harmony memories. A parameter called harmony memory acceptance rate, $r_{acceptance}$ is generally employed for the efficient utilization of harmony memory. The values of $r_{acceptance}$ range between 0 and 1. However, a typical range of $0.7 \sim 0.95$ is usually preferred for practical applications (Yang, 2009) because too small value of this parameter may result in the inclusion of only few best harmonies in the harmony memory and may cause slow convergence of the algorithm. On the other hand, a higher value of $r_{acceptance}$ leads to the use of most of the harmonies in the harmony memory leaving the other harmonies quite unexplored that may provide with the incorrect solutions.

The pitch adjustment component is determined by two parameters: band width of the pitch (b_{pitch}), and rate of pitch adjustment ($r_{PitchAdjustment}$). In music, adjustment of pitch typically refers to frequency change. Likewise, in HS algorithm, pitch adjustment refers to create a somewhat different solution (Geem et al., 2001).

The randomization component helps in increasing and maintaining the diversity of the HS solutions. This component is employed to further improve the search space by broaden the search space because pitch adjustment is primarily associated with certain local pitch adjustment that drives the algorithm to perform local search only. The addition of randomization component helps the HS algorithm in exploring a number of different diverse solutions, thus helping the algorithm in finding a solution which is very close to the global optimal solution.

The HS algorithm performs search of the optimal solutions through the utilization of four major steps:

- Step 1: Initialization of the HS memory, which contains a particular number of arbitrarily generated initial solutions.
- Step 2: Improvisation of a new solution from the initial HS memory.
- Step 3: Updating of the HS memory and evaluation of the new solution in step 2. If the new solution provides with the better objective function value for the considered optimization problem, the solution is kept. If the solution resulted in worse objective function value, the solution is discarded from the HS memory.
- Step 4: Repetition of steps 2 and 3 until the termination criterion (user-defined) is reached.

2.3.11. Imperialist Competitive Algorithm (ICA)

The ICA, introduced by Atashpaz-Gargari and Lucas (2007), is based on the theory of swarm intelligence dealing with both the continuous and discrete optimization problems. This metaheuristic algorithm is inspired by the principle of human social evolution strategy, i.e., the socio-political behaviors of human beings. Like other evolutionary algorithms, the ICA begins with a randomly generated initial population in which each individual population denotes a country in the world. In this initialization stage, few of the best countries (with lower value of cost function) in the population are selected as the 'imperialists' while the remainders of the population are used to form the 'colonies' of the selected imperialists. According to their power, all of the colonies obtained from the initial population are distributed among the

imperialists. Once the colonies are distributed among the imperialists, the colonies move toward their relevant imperialist country within the decision space. In ICA, the power of an empire is considered to be inversely proportional to its cost. The total power of an empire is calculated by adding the power of an imperialist country to a certain percentage of average power of the imperialist countries' colonies (Atashpaz-Gargari and Lucas, 2007). At this stage, all the empires are participated in the imperialistic competition. An empire is eliminated from the competition if it is unsuccessful in this competition, i.e., if it is unable to enhance its power or avoid deteriorating its power. As a result of this imperialistic competition, powerful empires gradually enhance their power while the less powerful empires lose their existing power and eventually collapse. The interaction among the colony movement toward the relevant imperialist countries, imperialistic competition, and the collapse mechanism ultimately cause all countries to a state of convergence where only one empire exists in the world and the other countries are regarded as the colonies of that empire. The execution of the ICA is accomplished using several stepwise procedures (Atashpaz--Gargari and Lucas, 2007). These steps include: (a) Creating initial empires (initialization), (b) Moving the colonies of an empire toward the imperialist (assimilation process), (c) Swapping the positions of an imperialist and a colony, (d) Calculating total power of an empire, (e) Imperialistic competition, (f) Eliminating the empires with less power, and (g) Convergence.

2.3.12. *Invasive Weed Optimization (IWO)*

The IWO, first introduced by Mehrabian and Lucas (Mehrabian and Lucas, 2006), is a population-based, derivative free and stochastic meta-heuristic optimization algorithm inspired by the colonizing behavior of weeds. Weeds are known to be very resistant to environmental vicissitudes and are able to adapt easily to climatic variabilities. Therefore, the growth of weeds is a serious threat to crop production. These characteristics of weeds, i.e., resistance and adaptability to adverse climatic conditions as well as the randomness of a weed community are incorporated into an optimization formulation, which intends to obtain an optimal solution of a mathematical function through mimicking the characteristics of a weed colony. The IWO algorithm is based on three major iterative processes such as reproduction, spatial dispersal, and competitive deprivation. It incorporates some of the basic features (seeding, growth, competition etc.) of a weed colony in order to converge to a global optimal solution of an optimization problem. In IWO, a solution of a particular optimization problem is referred to as a weed, and all weeds participates in the reproduction process. However, the fertility rates of these weeds are different, therefore, the numbers of seed produced by different weeds are also different. The seed production rate of a certain weed depends on the vigor and strength of that particular weed. This vigor and strength are referred to as 'fitness' of a weed in IWO algorithm. The seeds of weed are scattered randomly in the search space with a normal distribution of zero mean and an adaptive standard deviation. The reproduction phase is followed by a competition between weeds with their produced seeds. The weeds with higher fitness (produced more seeds) enter into the next generation.

In IWO, the habitat behavior of weeds is simulated through considering the following five processes or steps:

Step 1: Initialize primary population - In this step, a restrained quantity of seeds is distributed in the search domain.

Step 2: Reproduction - All of the seeds are allowed to grow and pass through the vegetative, flowering, and seed formation stages in order to produce seeds that depend on the fitness value of the individual weeds. The weeds with higher fitness value produce more seeds and those with lower fitness value produce less seeds.

Step 3: Spatial dispersal - The distribution of seeds around their parent weeds follows a normal distribution with zero mean and adaptive standard deviation. An adaptive standard deviation is employed to reduce the probability of dropping a seed in a distant area at each iteration as the algorithm proceeds. This adaptive conversion ensures the probability of seed falling at a distant area decreases nonlinearly at each iteration and assures the incorporation of more fit plants and elimination of less appropriate plants to the next generation.

Step 4: Competitive deprivation- Each weed with their seeds is integrated to form a population for the next generation. If the number of weeds surpasses the maximum number of weeds in the colony, the weeds with lower fitness values are eliminated from the colony in order to maintain a constant number of weeds in the colony. Nevertheless, the mechanism of reproduction and competition provide a chance to the weeds with lower fitness for reproduction. If they are able to reproduce more fit offspring, the generated offspring will have a chance to take part in the competition.

Step 5: Stopping criterion - The process continues, i.e., steps 2–4 is repeated until a user-defined stopping criterion (maximum number of iterations or objective function value) is reached. Once the stopping criterion is attained, the results with the minimum value of the objective function is stored.

2.3.13. *Particle Swarm Optimization (PSO)*

The PSO (Kennedy and Eberhart, 1995), a population-based stochastic optimization algorithm, is inspired by the social and psychological principles. The PSO is associated with the principles of swarm intelligence, which simulates the social behavior of bird flocking or fish schooling predation. The algorithm has gained popularity due to the possession of many advantageous characteristics such as it has a simple structure, robust maneuverability, and easy realization (Sun et al., 2019) that facilitates the training of various intelligent models. In PSO, every particle is regarded as a feasible solution within the search space of an optimization problem. On the other hand, the flight behavior of the particles is recognized as the search process of all individuals. In PSO, the dynamic update of the velocity of particles is determined by the past optimal location of the particle and the swarm population.

In PSO, the particle's objective function values are considered to be the corresponding fitness values. These fitness values determine the optimal position of the particles. The fitness values are also used to update the past most favourable location of the particles and optimal location of the swarm population. The control parameters of the PSO algorithm determine the convergence of particles trajectories (Sun et al., 2019). Convergence of the PSO algorithm is attained through maintaining a record of individual best fitness values of all particles, locating the global best particle, and bringing up-to-date location and velocity of each particle. In the event that the convergence is not attained, the iterative process continues until the optimization problem converges to its optimal solution or the maximum number of iterations is reached.

2.3.14. *Simulated Annealing (SA)*

The SA algorithm, an iterative metaheuristic search algorithm which mimics the slow cooling process of metals, was first introduced as a search engine for combinatorial optimization problems (Cerny, 1985; Kirkpatrick et al., 1983). The SA optimization approach adopts the principle of physical processes of heating and slow cooling of a material to minimize the damages or defects of that material. This physical heating and cooling processes eventually lead to the minimization of overall system energy. In SA, the efficient search is ensured by inclusion of a temperature schedule through generalization of the Metropolis Monte Carlo integration algorithm (Metropolis et al., 1953) by the Kirkpatrick algorithm (Kirkpatrick et al., 1983). Afterwards, the proof of sufficiency was demonstrated (Geman and Geman, 1984) by assigning a lower bound of $1/\log(t)$ to this temperature schedule. Here, t refers to an artificial measure of time of the annealing schedule. Nevertheless, the present form of SA algorithm is the outcome of the individual contributions of a number of scientists (Pincus, 1970). These contributions can be grouped into three main categories (Ingber, 1996): Boltzmann annealing (BA), simulated quenching (SQ), and fast annealing (FA). A brief description of each of these categories are presented below:

2.3.14.1. Boltzmann annealing (BA). The first SA was based on a Monte Carlo importance-sampling technique intended to solve large-dimensional path integrals related to the problems of statistical physics (Metropolis et al., 1953).

2.3.14.2. Simulated quenching (SQ). Although SA has become an attractive optimization algorithm due to its easy implementation and flexibility to handle complex objective functions and constraints, the computational burden in terms of long execution time has been a real challenge for the utilization of standard Boltzmann-type SA (Ingber, 1996). This necessitates the incorporation of a temperature schedule, which is consistent with the Boltzmann algorithm and at the same time fast enough to meet the 'sufficiency conditions' needed to bring about an exact (weak) ergodic exploration of solutions. A logarithmic temperature schedule is convinced to be consistent with the Boltzmann algorithm. An exponential temperature schedule may also be used with the Boltzmann algorithm. However, the use of exponential temperature schedule is well-justified in an adaptive simulated annealing (a variant of SA) provided the use of a particular distribution is ensured for the generating function (Ingber, 1989).

2.3.14.3. Fast annealing (FA). Up until 1987, much attention was not paid to search for alternative algorithms other than the development of various variants and improvement made on the standard Boltzmann algorithm (van Laarhoven et al., 2020). It was Szu and Hartley (1987), who pointed out that a Cauchy distribution is able to provide several certain advantages over the Boltzmann algorithm. For instance, it has a 'fatter' tail when compared to the Gaussian form of the Boltzmann distribution, which allows identifying and testing the local optima in the search process for the anticipated global optima.

The working principle of SA algorithm starts with generating a new point, i.e., the SA algorithm randomly generates a new point at each iteration. The search domain is determined by the distance between the randomly generated new point and the present point. As discussed above, a probability distribution (Cauchy or Gaussian) whose scale is proportional to the 'temperature' determines the degree of search. The SA algorithm accepts not only all new points that minimize the objective function value but also other particular points (with a certain probability level) that raise the objective function value. This acceptance of points that raise the objective function value is performed to allow exploration of more plausible solutions which leads to finding the global optimal solutions. Another advantage is that the inclusion of more points avoids the SA algorithm to be trapped in the local optima. As execution of the algorithm proceeds, an 'annealing schedule' is designated to decrease the 'temperature' systematically. The extent of search process is reduced with the decrease in 'temperature' until the algorithm converges to a global optimal solution.

2.3.15. Teaching-Learning-based Optimization (TLBO)

The TLBO, proposed by Rao et al. (2011), is a population-based metaheuristic search algorithm. It utilizes a population of solutions to converge to the global optimal solutions. The population in TLBO represents a group of students or a class of learners. The teaching and learning processes in a classroom environment form the basic principle of the TLBO algorithm. It deals with the significances of influence of a teacher on learners in a classroom environment. The algorithm is associated with two major phases: 'Teacher Phase', and 'Learner Phase'. The 'Teacher Phase' deals with learning of the learners from the teachers while the 'Learner Phase' deals with the learning process through interaction among the learners. Four step-wise procedures as outlined in Rao et al. (2011) are utilized in the implementation of TLBO algorithm. These are: (a) Problem definition and parameter initialization (step 1), (b) Initialize population (step 2), (c) Teacher phase (step 3), (d) Learner phase (step 4). The details of these steps with the associated equations can be found in Rao et al. (2011), and are not repeated here.

Table 2
Activities in forward and backward passes during hybrid learning of ANFIS (Jang, 1993).

	Premise parameters	Consequent parameters	Signals
Forward pass	Fixed	Least Squares Estimate	Node outputs
Backward pass	Gradient Descent	Fixed	Error rates

2.3.16. Gradient Descent- Least Squares Estimate (GD-LSE) algorithm

The basic learning rules of an adaptive network are composed of two components: gradient descent and chain rule (Werbos, 1974). This gradient-based learning approach requires longer convergence time with the possibility of converging to local optima. To avoid these two disadvantages, Jang (1993) proposed a hybrid learning approach. This hybrid learning rule integrates the Gradient Descent (GD) method with the Least Squares Estimate (LSE) for tuning the parameters of adaptive networks to obtain optimal network parameters. This integration of two approaches is referred to as Gradient Descent- Least Squares Estimate (GD-LSE), which is utilized to tune the parameters of the proposed Sugeno type ANFIS model. The GD-LSE utilizes a forward and a backward pass to execute the hybrid learning procedure. In the forward pass, the functional signals are forwarded up to layer 4 of the ANFIS architecture, and then the LSE is employed to recognize the 'consequent parameters' while the 'premise parameters' are kept fixed. On the other hand, 'consequent parameters' are kept unchanged in the backward pass, and the 'premise parameters' are reorganized by the GD algorithm. Moreover, in the backward pass of the algorithm, the error rates propagate to the backward direction. The obtained 'consequent parameters' are regarded as optimum within the desired parameter space of the consequent parts when the 'premise parameters' are held unchanged. The learning procedure of the ANFIS architecture using hybrid algorithm can be summarized in Table 2.

3. ANFIS-optimization algorithm hybrid models

A total of 16 hybridized ANFIS models were developed whose parameters were tuned and optimized using the algorithms described in subsection "2.3 Optimization algorithms for tuning ANFIS parameters". Various parameters of the optimization algorithms were obtained through several trials in which the performances of the hybrid ANFIS models were carefully examined. The entire dataset was divided into training (80%), validation (10%), test (10%) sets. The Root Mean Squared Error (RMSE) values between the FAO-56 PM-calculated and the hybrid ANFIS model predicted ET_0 were used to evaluate the training performance of the developed ANFIS models. In addition, the validation RMSE values were used to check the model over- and under-training by observing the absolute differences between the training and validation RMSE values. The remaining 10% (used neither to train nor to validate the models) of the data was used to test the performances of the developed ANFIS models. Parameters of the optimization algorithms used to tune ANFIS parameters are presented in Table 3. The different maximum numbers of iterations used for the optimization algorithms ensured convergence of the particular algorithm.

4. Ranking of prediction models: weight assignment

Statistical performance evaluation indices were calculated on the test dataset for evaluating the performances of the developed optimization algorithm tuned ANFIS models. It is noted that different ANFIS models may have conflicting performances with respect to various performance indices, i.e., one model may be considered as superior when RMSE criterion is used while another model may be regarded as the best performer when MAD criterion is used. Decision making in such situations is difficult and deciding on the best performing model is often impossible when a set of different performance indices are employed. In these situations, decision theories that incorporate various performance

Table 3
Optimal parameter values for the optimization algorithms.

Algorithms	Optimal parameter values	
ABC	Maximum number of iterations: 200 Population size: 100 Number of onlooker bees: 100 Abandonment limit parameter: 0.6 × number of variables × population size Upper bound of acceleration coefficient: 1	
BA	Maximum number of iterations: 200 Population size: 100 Number of selected sites: 0.5 × population size Number of selected elite sites: 0.4 × number of selected sites Number of recruited bees for selected sites: 0.5 × population size Number of recruited bees for elite sites: 2 × number of recruited bees for selected sites Neighbourhood radius: 0.1 × (Maximum value of variable – Minimum value of the variable) Neighbourhood radius damp rate: 0.95	
BBO	**BBO settings** Maximum number of iterations: 1000 Population size: 200 Keep rate: 0.2 Number of kept habitats: Keep rate × Population size = 40 Number of new habitats: Population size – Number of inhabitants kept = 160 **Migration rates** Emigration rates: A linearly spaced vector of 200 points. The spacing between the points = (1-0)/(200-1) Immigration rates: 1 – Emigration rates Alpha: 0.9 Mutation: 0.1 Sigma: 0.2	
ACOR & CA	**ACOR** Maximum number of iterations: 1000 Population size: 100 Sample size: 40 Intensification factor (selection pressure): 0.5 Deviation-distance ratio: 1	**CA** Maximum number of iterations: 200 Population size: 100 Acceptance ratio: 0.35 Number of accepted individuals: Acceptance ratio × Population size Alpha: 0.3 Beta: 0.5
CMAES	Maximum number of iterations: 300 Population size (and number of offspring): lambda = (4 + round (3 × log (number of variables)) × 10 Number of parents: mu = round (lambda / 2)	
DE & FA	**DE** Maximum number of iterations: 1000 Population size: 100 Lower bound of scaling factor: 0.2 Upper bound of scaling factor: 0.8 Crossover probability: 0.2	**FA** Maximum number of iterations: 500 Number of fireflies (Swarm Size): 100 Light absorption coefficient: 1 Attraction coefficient base value: 2 Mutation coefficient: 0.2 Mutation coefficient damping ratio: 0.98 Uniform mutation range: 0.5
GA	Maximum number of iterations: 200 Population size: 100 Crossover percentage: 0.4 Number of offspring (parents): 2 × round (crossover percentage × population size / 2) Mutation percentage: 0.7 Number of mutants: round (mutation percentage × population size) Gamma: 0.7 Mutation rate: 0.15 Selection pressure: 8	
HA	Maximum number of iterations: 200 Harmony memory size (population size): 100 Number of new harmonies: 20 Harmony memory consideration rate: 0.9 Pitch adjustment rate: 0.1 Fret width (bandwidth): 0.02 × (Maximum value of variable – Minimum value of the variable) Fret width damp ratio: 0.995	
ICA & IWO	**ICA** Maximum number of iterations: 1000 Population size: 100 Number of empires/imperialists: 10 Selection pressure: 1 Assimilation coefficient: 1.5 Revolution probability: 0.05 Revolution rate: 0.1 Colonies mean cost coefficient: 0.2	**IWO** Maximum number of iterations: 300 Population size: 100 Minimum number of seeds: 0 Maximum number of seeds: 5 Variance reduction exponent: 2 Initial value of standard deviation: 0.5 Final value of standard deviation: 0.001
PSO & SA	**PSO** Maximum number of iterations: 200 Population size (Swarm size): 100 Inertia weight: 1 Inertia weight damping ratio: 0.99	**SA** Maximum number of iterations: 200 Maximum number of sub-iterations: 10 Population size: 20 Initial temperature: 0.025

(*continued on next page*)

Table 3 (*continued*)

Algorithms	Optimal parameter values	
	Personal learning coefficient: 1	Temperature reduction rate: 0.99
	Global learning coefficient: 2	Number of neighbours per individual: 5
	Maximum velocity: 1	
	Minimum velocity: -1	
TLBO	TLBO typically does not necessitate any algorithm parameters to be tuned (Rao et al., 2011)	
	Maximum number of iterations: 2000	
	Population size (Swarm size): 20	
GD-LSE	**FIS parameters**	**ANFIS parameters**
	Fuzzy partition matrix exponent: 1.1	Maximum number of Epochs: 200
	Maximum number of iterations: 200	Error goal: 0
	Minimum improvement: 1×10^{-5}	Initial step size: 0.01
		Step size decrease rate: 0.9
		Step size increase rate: 1.1

evaluation indices often provide a better insight of selecting the best model. SE, VC, and GRA-based decision theories have successfully been utilized in different research domains for uncertainty quantification and selection of best alternatives from a set of different feasible alternatives (Chen, 2019; Li et al., 2019, 2011; Luo et al., 2016; Roy and Datta, 2019, 2018; Xu and Xu, 2018). The present study applied these decision theories in order to provide a ranking of the optimization algorithm tuned ANFIS models for predicting daily ET_0. For this, eight performance evaluation indices were calculated: Correlation Coefficient (R), Nash-Sutcliffe Efficiency Coefficient (NS), Willmott's Index of Agreement (IOA), Kling-Gupta Efficiency (KGE), Maximum Absolute Error (MAE), Median Absolute Deviation (MAD), Root Mean Squared Error (RMSE), and Normalized RMSE (NRMSE). Among them, four benefit indices (the higher the better: R, NS, IOA, KGE) and four cost indices (the lower the better: MAE, MAD, RMSE, NRMSE) were used in this study to rank the performances of the developed prediction models.

The first step of weight assignment is associated with developing a decision matrix of prediction models and performance evaluation indices. Assume that there are m prediction models and PEI performance evaluation indices such that the decision matrix can be expressed by the following equation (Wu et al., 2011):

$$ET_{ij} = \begin{bmatrix} ET_{11} & ET_{21} & \cdots & ET_{m1} \\ ET_{12} & ET_{22} & \cdots & ET_{m2} \\ \vdots & \vdots & \vdots & \vdots \\ ET_{1PEI} & ET_{2PEI} & \cdots & ET_{mPEI} \end{bmatrix} \tag{25}$$

The next step is to standardize the decision matrix to minimize the effects of index dimensionality. The values of performance indices were standardized between 0 and 1 such that $S_{ij} \in [0,1],\ i = 1,2,\ldots,m; j = 1,2,\ldots,PEI$. S_{ij} is expressed as (Wu et al., 2011):

$$S_{ij} = \begin{cases} \dfrac{ET_{ij}}{\max(ET_{i1}, ET_{i2}, \ldots, ET_{iPEI})}, & \textit{for benefit indices} \\ \dfrac{X_{ij}}{\min(ET_{i1}, ET_{i2}, \ldots, ET_{iPEI})}, & \textit{for cost indices} \end{cases} \tag{26}$$

4.1. Entropy weight

Entropy weights to individual prediction model were assigned using the Entropy-based ranking of the models. The ranking was performed by the following steps (Li et al., 2011):

Step1: Computation of each index's Entropy value using the concepts of Shannon's information Entropy. Entropy value of the j^{th} index was calculated as

$$Entropy_j = -k\sum_{i=1}^{m} f_{ij}\ln f_{ij} \tag{27}$$

where,

$$f_{ij} = S_{ij} \Big/ \sum_{i=1}^{m} S_{ij} \tag{28}$$

$$k = 1/\ln m \tag{29}$$

Step2: Calculation of each index's Entropy weight. j^{th} index's entropy weight was calculated by:

$$w(entropy)_j = \frac{1 - Entropy_j}{PEI - \sum_{j=1}^{PEI} Entropy_j} \tag{30}$$

This Entropy weight indicates the importance of the index in the decision-making process. The higher the value of Entropy based weight, the more information the particular index carries, and more significant this index is in the decision-making.

Step3: Calculation of each model's ranking weight by summing up the product of each index's Entropy weight and the standardized value of that index. This step is mathematically represented by

$$w(entropy)_i = \sum_{j=1}^{PEI} S_{ij} \times w(entropy)_j \tag{31}$$

Step4: Determination of model ranking

$$\max \quad [w(entropy)_i], \ldots., \min[w(entropy)_i]; \text{for } i = 1,2,\ldots, \quad m \tag{32}$$

Step5: Calculation of Entropy weight for individual prediction models

$$W(entropy)_i = w(entropy)_i \Big/ \sum_{i=1}^{m} w(entropy)_i \tag{33}$$

4.2. Variation Coefficient weight

Variation Coefficient (VC) weights to individual prediction model were assigned using the VC based ranking of the models. The ranking was performed by the following steps (Zhang and Xie, 2010).

Step1: Calculation of the mean values of the j^{th} index

$$\overline{s_j} = \frac{1}{m}\sum_{i=1}^{m} S_{ij} \tag{34}$$

Step2: Calculation of the mean squared error of the j^{th} index

$$MSE_j = \sqrt{\frac{1}{m}\sum_{i=1}^{m}\left(S_{ij} - \overline{s_j}\right)^2} \tag{35}$$

Step3: Calculation of the Coefficient of Variation of the j^{th} index

$$VC_j = MSE_j \big/ \overline{s_j} \tag{36}$$

Step4: Calculation of each index's VC weight. VC weight of the j^{th} index is given by:

$$w(VC)_j = VC_j \Big/ \sum_{j=1}^{PEI} VC_j;\ \sum_{j=1}^{PEI} w(VC)_j = 1 \tag{37}$$

Step5: Calculation of each model's ranking weight by summing up the product of each index's VC weight and the standardized value of that index. This step is mathematically represented by

$$w(VC)_i = \sum_{j=1}^{PEI} S_{ij} \times w(VC)_j \tag{38}$$

Step6: Determination of model ranking

$$\max \quad [w(VC)_i], \ldots, \min[w(VC)_i]; \text{for } i = 1, 2, \ldots, \quad m \tag{39}$$

Step7: Calculation of VC weight for individual prediction models

$$W(VC)_i = w(VC)_i \Big/ \sum_{i=1}^{m} w(VC)_i \tag{40}$$

4.3. Grey Relational Analysis weight-based ensemble

Gray Relational Grade (GRG) approach as implemented in Wang and Rangaiah (2017) was used in this study to provide a prioritization of the prediction models. The GRG approach utilizes the resemblance between the performance index values of individual prediction models and the ideal or the best reference performance index values. The GRG is calculated using the following steps (Wang and Rangaiah, 2017):

Step 1: Standardize the performance index values for eliminating the effects of dimensionality. For benefit indices, standardization was calculated using the following equation:

$$ET_{ij} = \frac{ET_{ij} - \min_{i \epsilon m} ET_{ij}}{\max_{i \epsilon m} ET_{ij} - \min_{i \epsilon m} ET_{ij}} \tag{41}$$

For the cost indices, standardization was performed as:

$$ET_{ij} = \frac{\max_{i \epsilon m} ET_{ij} - ET_{ij}}{\max_{i \epsilon m} ET_{ij} - \min_{i \epsilon m} ET_{ij}} \tag{42}$$

Step 2: Find the ideal or best reference performance index values

$$ET_j^{Ideal} = \max_{i \epsilon m} ET_{ij} \tag{43}$$

Step 3: Obtain the deviation between the ET_j^{Ideal} and ET_{ij}

$$\Delta D_{ij} = \left| ET_j^{Ideal} - ET_{ij} \right| \tag{44}$$

Step 4: Calculate GRG values for each prediction model:

$$GRG_i = \frac{1}{m} \sum_{j=1}^{PEI} \frac{\Delta\min + \Delta\max}{\Delta D_{ij} + \Delta\max} \tag{45}$$

where, i = index of the number of prediction models ($i = 1, 2, \ldots, m$), j = the index of the number of performance indices ($j = 1, 2, \ldots, PEI$), $\Delta\max = \max_{i \epsilon m, j \epsilon PEI}(\Delta D_{ij})$, $\Delta\min = \min_{i \epsilon m, j \epsilon PEI}(\Delta D_{ij})$.

Based on the concept of Gray Relational Analysis, the larger the value of GRG_i the more reliable the prediction model is. Therefore, the largest value of GRG_i is the recommended best prediction model among all the prediction models.

5. Performance evaluation of the developed models

The following performance evaluation indices were calculated on the test dataset to evaluate the performance of the developed optimization algorithm tuned ANFIS models:

Correlation Coefficient, R

$$R = \frac{\sum_{i=1}^{n} \left(ET_{i,a} - \overline{ET_a}\right)\left(ET_{i,a} - \overline{ET_p}\right)}{\sqrt{\sum_{i=1}^{n} \left(ET_{i,a} - \overline{ET_a}\right)^2} \sqrt{\sum_{i=1}^{n} \left(ET_{i,p} - \overline{ET_p}\right)^2}} \tag{46}$$

Normalized Root Mean Square Error, NRMSE (%)

$$NRMSE = \frac{RMSE}{\overline{ET_a}} \times 100 = \frac{\sqrt{\frac{1}{n} \sum_{i=1}^{n} \left(ET_{i,a} - ET_{i,p}\right)^2}}{\overline{ET_a}} \times 100 \tag{47}$$

Maximum Absolute Error, MAE

$$MAE = \max \left[\left| ET_{i,a} - ET_{i,p} \right| \right] \tag{48}$$

Median Absolute Deviation, MAD

$$MAD(ET_a, ET_p) = median\left(\left|ET_{1,a} - ET_{1,p}\right|, \left|ET_{2,a} - ET_{2,p}\right|, \ldots, \left|ET_{n,a} - ET_{n,p}\right|\right)$$

$$for\ i = 1, 2, \ldots, n \tag{49}$$

Nash-Sutcliffe Efficiency Coefficient, NS

$$NS = 1 - \frac{\sum_{i=1}^{n} \left(ET_{i,a} - ET_{i,p}\right)^2}{\sum_{i=1}^{n} \left(ET_{i,a} - \overline{ET_a}\right)^2} \tag{50}$$

Kling–Gupta Efficiency, KGE

$$KGE = 1 - ED = 1 - \sqrt{(R-1)^2 + (\propto - 1)^2 + (\beta - 1)^2} \tag{51}$$

$$\propto = \frac{\sqrt{\frac{1}{n} \sum_{i=1}^{n} \left(ET_{i,p} - \overline{ET_p}\right)^2}}{\sqrt{\frac{1}{n} \sum_{i=1}^{n} \left(ET_{i,a} - \overline{ET_a}\right)^2}} \tag{52}$$

$$\beta = \frac{\frac{1}{n} \sum_{i=1}^{n} ET_{i,p}}{\frac{1}{n} \sum_{i=1}^{n} ET_{i,a}} \tag{53}$$

where, $ET_{i,a}$ and $ET_{i,p}$ are ET_0 values at the i^{th} step obtained by FAO-56 PM and ANFIS models, respectively, n = number of data points, $\overline{ET_a}$ is the mean value of the FAO-56 PM ET_0 values, ED = Euclidian distance from the ideal data points, $\propto$ = relative variability in the predicted and simulated ET_0values, β = ratio between the mean predicted and mean simulated ET_0values representing the bias.

In addition, a recently proposed engineering index, $a^{10} - index$, was calculated to assess the reliability of the developed prediction models

$$a^{10} - index = \frac{\mathscr{E}^{10}}{\mathscr{L}} \tag{54}$$

where, $\mathscr{L}$ is the number of test datasets and $\mathscr{E}^{10}$ is the number of test samples that have a *Actual* /*Predicted* value between 0.90 and 1.10. Note that for a perfect predictive model, the values of $a^{10} - index$ are expected to be unity. The proposed $a^{10} - index$ has the advantage that their value has a physical engineering meaning. It represents the amount of the samples that satisfies predicted values with a deviation of ± 10% compared to actual values (FAO-56 PM estimated ET_0 values in this study).

6. Results

In this study, optimization algorithm tuned ANFIS models were used to predict ET_0 time series computed using FAO-56 PM equation for the considered meteorological station. For this, several approaches were used, e.g., classical ANFIS model (GD-LSE-ANFIS), optimization

Table 4
Cross-correlation coefficients between ET_0 and input variables.

Variables	ET_0, mm/d
Minimum temperature, ^{0}C	0.5124
Maximum temperature, ^{0}C	0.7740
Relative humidity, %	-0.4118
Wind speed, km/d	0.6236
Sunshine hours, h	0.5688

algorithm tuned ANFIS models, and three decision theories (SE, VC, and GRA). The performances of all developed ANFIS models were evaluated using several statistical performance evaluation indices.

Five climatic variables such as minimum and maximum air temperatures, relative humidity, wind speed, and sunshine hours were used as inputs to the hybrid ANFIS models. This selection of input variables was performed by observing cross-correlation values between the input variables and the calculated ET_0 values. The calculated cross-correlation values of similar magnitude between the input variables and the resulting ET_0 values indicated that all input variables contributed to a similar extent in calculating ET_0 values. The cross-correlation values are presented in Table 4. The highest positive value of 0.774 indicated that the maximum temperature had the greatest impact on determining the ET_0, whereas relative humidity had the lowest influence (the negative value of − 0.412). It is agreed that using maximum possible inputs usually provide the best prediction results (Tao et al., 2018). As such, all input variables were used in developing the hybrid ANFIS models.

The Fuzzy C-Mean Clustering (FCM) (Bezdek et al., 1984) algorithm was used to divide the input datasets into identical clusters in the training of ANFIS models. The optimum numbers of clusters that provided the best training and validation performance were decided upon conducting trials in which the numbers of clusters ranged between 2 and 5. The trial was limited to 5 clusters because increasing the numbers of clusters did not improve the training performance significantly while incurred an increased computational time requirement. An ANFIS model with a particular number of clusters was selected by observing the training and validation RMSE values as well as the absolute differences in RMSE values between training and validation phases of model development. A model was selected when both training and validation RMSE as well as their absolute differences were minimum. Training and validation RMSE values of different optimization algorithm tuned ANFIS models for different numbers of clusters are presented in Table 5. It is observed from Table 5 that ANFIS models bearing 3, 2, 2, 2, 2, 3, 2, 4, 4, 2, 3, 2, 3, 2, 4, 2 clusters were observed to be optimal when tuned with ABC, BA, BBO, ACOR, CMAES, CA, DE, FA, GA, HS, ICA, IWO, PSO, SA, TLBO, and GD-LSE, respectively. Although training time was not considered as a selection criterion, the time required to train the models with varying numbers of clusters was calculated and is presented in Table 6.

Table 6
Training time required to develop different optimization algorithm tuned ANFIS models with respect to different numbers of clusters.

Algorithms	Time taken, sec			
	Two clusters	Three clusters	Four clusters	Five clusters
ABC	1686	1454	1694	1682
BA	19,143	19,845	22,631	27,378
BBO	4535	6389	6443	7606
ACOR	5386	2388	2256	1779
CMAES	961	1357	1631	2007
CA	1074	1282	905	1050
DE	2167	2676	3298	3858
FA	53,230	67,029	84,587	98,838
GA	979	637	732	857
HS	463	587	689	801
ICA	2384	2905	3395	3974
IWO	754	931	1186	1429
PSO	441	551	667	781
SA	4560	5667	6663	8075
TLBO	1915	2366	2657	3252
GD-LSE	9	12	18	19

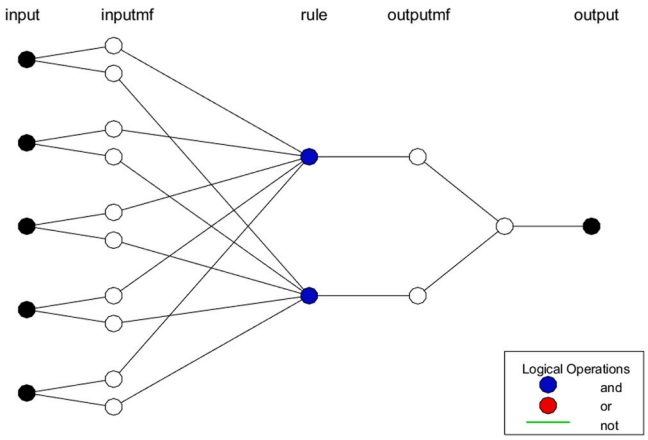

Fig. 4. ANFIS predictive model structure with two input membership functions for each of the five inputs.

ANFIS architectures with two (BA, BBO, ACOR, CMAES, DE, HS, IWO, SA, and HA tuned ANFIS), three (ABC, CA, ICA, and PSO tuned ANFIS), and four (FA, GA, and TLBO tuned ANFIS) clusters are shown in Figs. 4, 5, and 6, respectively.

Table 5
Training and validation RMSE of different optimization algorithm tuned ANFIS models with different numbers of clusters.

Algorithms	Two clusters		Three clusters		Four clusters		Five clusters	
	Train	Validation	Train	Validation	Train	Validation	Train	Validation
ABC	0.313	0.282	0.303	0.275	0.314	0.287	0.317	0.289
BA	0.276	0.257	0.297	0.312	0.283	0.327	0.315	0.287
BBO	0.169	0.170	0.165	0.170	0.169	0.171	0.167	0.174
ACOR	0.315	0.286	0.315	0.286	0.315	0.286	0.315	0.286
CMAES	0.240	0.238	0.315	0.291	0.318	0.288	0.330	0.297
CA	0.743	0.771	0.307	0.290	0.305	0.278	0.302	0.352
DE	0.240	0.237	0.272	0.235	0.266	0.511	0.312	0.283
FA	0.162	0.161	0.154	0.177	0.155	0.156	0.154	0.199
GA	0.199	0.212	0.214	0.231	0.229	0.230	0.254	0.234
HS	0.242	0.242	0.292	0.281	0.296	0.274	0.290	0.279
ICA	0.177	0.184	0.164	0.168	0.210	0.201	0.201	0.210
IWO	0.227	0.252	0.314	0.284	0.295	0.270	0.315	0.286
PSO	0.163	0.166	0.161	0.162	0.154	0.158	0.158	0.163
SA	0.200	0.202	0.242	0.468	0.223	0.251	0.200	0.202
TLBO	0.177	0.182	0.211	0.226	0.178	0.180	0.241	0.728
GD-LSE	0.162	0.164	0.157	0.176	0.157	0.165	0.147	0.152

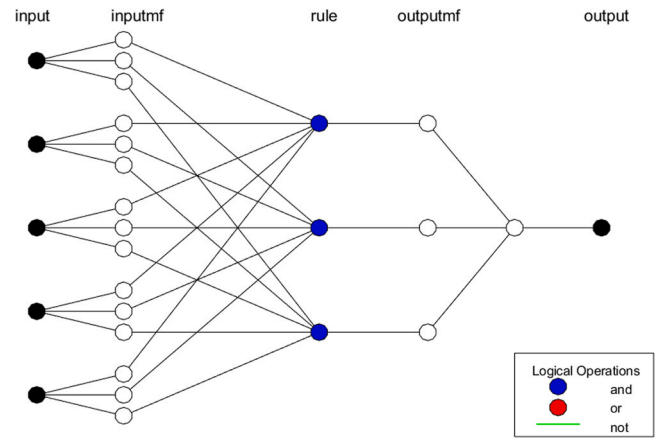

Fig. 5. ANFIS predictive model structure with three input membership functions for each of the five inputs.

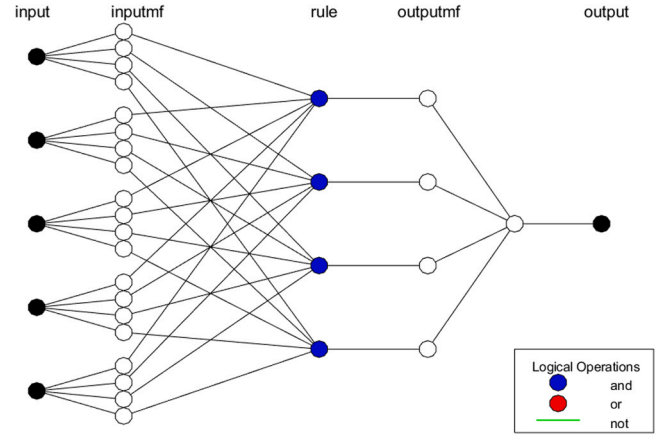

Fig. 6. ANFIS predictive model structure with four input membership functions for each of the five inputs.

The time required to train and validate the various ANFIS models presented in Table 6 revealed that the implementation of GD-LSE significantly reduced the time required for ANFIS training. It is also observed from Table 6 that, in general, the required training time increased with an increase in the number of clusters for the proposed optimization algorithms and that the FA algorithm required the greatest training time followed by BA, BBO, SA, and so on.

The performance evaluation results are presented in the form of absolute error box plots. Fig. 7 illustrates box plots of absolute errors between FAO-56 PM estimated and model predicted ET_0 values produced by different optimization algorithm tuned ANFIS models denoted by M1–M16 (M1 = ABC-ANFIS, M2 = ACOR-ANFIS, M3 = GD-LSE-ANFIS, M4 = BA-ANFIS, M5 = BBO-ANFIS, M6 = CA-ANFIS, M7 = CMAES-ANFIS, M8 = DE-ANFIS, M9 = FA-ANFIS, M10 = GA-ANFIS, M11 = HS-ANFIS, M12 = ICA-ANFIS, M13 = IWO-ANFIS, M14 = PSO-ANFIS, M15 = SA-ANFIS, M16 = TLBO-ANFIS). Horizontal line inside each box in Fig. 7 indicates the median of the absolute error between the FAO-56 PM estimated and model predicted ET_0 for the particular prediction model. The black circle denotes the mean of the absolute errors and '×' symbols represent outliers. It is perceived from Fig. 7 that minimum values of the absolute error mean (0.113 mm/d) and median (0.082 mm/d) were obtained from FA-ANFIS indicating the superior performance of the FA-ANFIS model over others based on the absolute error criterion. On the other hand, CA-ANFIS produced the maximum mean value (0.236 mm/d) of absolute errors whereas ACOR-ANFIS produced the maximum median value (0.192 mm/d) of absolute errors. In sum, the results revealed the superior performance of FA to considerably enhance the prediction capabilities of ANFIS for the considered application presented in this study.

In addition, the performances of the proposed optimization algorithm tuned ANFIS models in predicting ET_0 were evaluated using various statistical performance evaluation indices (as described in Section 5). The performance results are presented in Table 7. In quantitative terms, FA-ANFIS model provided the best results for most of the performance evaluation indices (R = 0.993, NS = 0.986, IOA = 0.996, KGE = 0.989, MAD = 0.054 mm/d, RMSE = 0.149 mm/d, and NRMSE = 3.819%). On the other hand, CA-ANFIS produced the worst prediction accuracies (NS = 0.944, IOA = 0.984, KGE = 0.883, RMSE = 0.294 mm/d, NRMSE = 7.507%, and a^{10}-index = 0.792) when

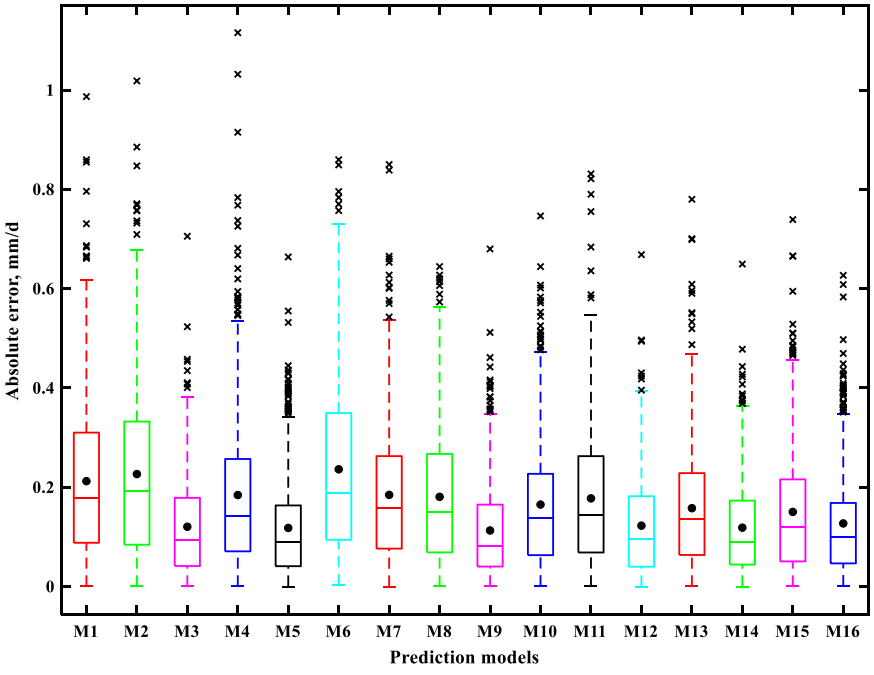

Fig. 7. Box plots of absolute errors between FAO-56 PM estimated and model predicted ET_0 values. M1 = ABC-ANFIS, M2 = ACOR-ANFIS, M3 = GD-LSE-ANFIS, M4 = BA-ANFIS, M5 = BBO-ANFIS, M6 = CA-ANFIS, M7 = CMAES-ANFIS, M8 = DE-ANFIS, M9 = FA-ANFIS, M10 = GA-ANFIS, M11 = HS-ANFIS, M12 = ICA-ANFIS, M13 = IWO-ANFIS, M14 = PSO-ANFIS, M15 = SA-ANFIS, and M16 = TLBO-ANFIS. Median of absolute errors are indicated by the horizontal lines inside each box. The black circles and × symbols denote the mean of absolute errors and the outliers, respectively.

Table 7
Performance statistics of all optimization algorithm tuned ANFIS models.

Model	R	NS	IOA	KGE	MAE, mm/d	MAD, mm/d	RMSE, mm/d	NRMSE, %	a^{10}-index
ABC-ANFIS	0.979	0.954	0.987	0.917	0.987	0.111	0.267	6.825	0.827
ACOR-ANFIS	0.975	0.947	0.986	0.923	1.018	0.116	0.285	7.290	0.793
GD-LSE-ANFIS	0.992	0.984	0.996	0.988	0.706	0.061	0.157	4.021	0.972
BA-ANFIS	0.981	0.962	0.990	0.977	1.116	0.089	0.242	6.191	0.841
BBO-ANFIS	0.992	0.984	0.996	0.980	0.664	0.056	0.158	4.027	0.936
CA-ANFIS	0.977	0.944	0.984	0.883	0.860	0.115	0.294	7.507	0.792
CMAES-ANFIS	0.984	0.965	0.991	0.948	0.850	0.091	0.232	5.917	0.853
DE-ANFIS	0.985	0.967	0.992	0.975	0.645	0.097	0.227	5.796	0.825
FA-ANFIS	0.993	0.986	0.996	0.989	0.680	0.054	0.149	3.819	0.965
GA-ANFIS	0.988	0.971	0.993	0.971	0.746	0.084	0.210	5.376	0.882
HS-ANFIS	0.983	0.966	0.991	0.963	0.831	0.093	0.228	5.821	0.882
ICA-ANFIS	0.992	0.983	0.996	0.983	0.669	0.064	0.161	4.104	0.947
IWO-ANFIS	0.987	0.974	0.993	0.983	0.780	0.079	0.200	5.117	0.910
PSO-ANFIS	0.992	0.985	0.996	0.986	0.650	0.057	0.153	3.913	0.968
SA-ANFIS	0.988	0.975	0.994	0.969	0.739	0.075	0.196	5.007	0.883
TLBO-ANFIS	0.991	0.982	0.995	0.985	0.627	0.056	0.168	4.280	0.924

compared with others. It is observed from Table 7 that FA-ANFIS was evidenced to be the best prediction model among the 16 individual models for most of the performance evaluation indices, except the IOA, MAE, and a^{10}-index for which PSO-ANFIS, TLBO-ANFIS, and GD-LSE-ANFIS showed the superior performance. In other words, IOA, MAE, and a^{10}-index criteria suggest the superiority of PSO-ANFIS, TLBO-ANFIS, and GD-LSE-ANFIS, respectively, among others. On the other hand, CA-ANFIS proved to be the worst performer for the six performance evaluation indices (NS, IOA, KGE, RMSE, NRMSE, and a^{10}-index). The performance of ACOR-ANFIS was found to be inferior with respect to R and MAD criteria whereas BA-ANFIS showed poor performance when MAD criterion was used. Consequently, it is apparent that the performances of different ANFIS models were ranked differently when different performance evaluation indices were computed based on the models' performance on test dataset. Decision making in such situations is quite difficult which can be easily overcome by applying a decision theory that considers several performance indices instead of relying on a single index. The contribution of several performance indices needs to be incorporated within a general framework of a decision tool in evaluating the superiority of a standalone prediction model compared to others.

In this effort, SE, VC, and GRA based decision theories described in section "4: Ranking of prediction models: weight assignment" were applied and the corresponding ranking values were computed to address the contrasting performances of the ANFIS models on different performance indices. SE, VC, and GRA based ranking results are shown in Table 8.

Table 8
Ranking of prediction models based on entropy, variation coefficient and Grey relational analysis weights.

Entropy weight		Variation Coefficient weight		Grey Relational Analysis weight	
Weights	Models	Weights	Models	Weights	Models
0.990	FA-ANFIS	0.988	FA-ANFIS	0.447	GD-LSE -ANFIS
0.984	PSO-ANFIS	0.969	PSO-ANFIS	0.445	FA-ANFIS
0.976	BBO-ANFIS	0.958	BBO-ANFIS	0.445	PSO-ANFIS
0.968	TLBO-ANFIS	0.934	TLBO-ANFIS	0.445	ICA-ANFIS
0.960	GD-LSE-ANFIS	0.921	GD-LSE -ANFIS	0.444	BBO-ANFIS
0.955	ICA-ANFIS	0.903	ICA-ANFIS	0.443	IWO-ANFIS
0.884	SA-ANFIS	0.763	SA-ANFIS	0.441	TLBO-ANFIS
0.872	IWO-ANFIS	0.736	IWO-ANFIS	0.440	GA-ANFIS
0.861	GA-ANFIS	0.711	GA-ANFIS	0.440	SA-ANFIS
0.854	DE-ANFIS	0.675	DE-ANFIS	0.437	DE-ANFIS
0.826	HS-ANFIS	0.648	HS-ANFIS	0.437	HS-ANFIS
0.821	CMAES-ANFIS	0.644	CMAES-ANFIS	0.434	CMAES-ANFIS
0.797	BA-ANFIS	0.610	BA-ANFIS	0.427	BA-ANFIS
0.768	ABC-ANFIS	0.551	ABC-ANFIS	0.423	ABC-ANFIS
0.759	CA-ANFIS	0.532	CA-ANFIS	0.416	ACOR-ANFIS
0.754	ACOR-ANFIS	0.522	ACOR-ANFIS	0.414	CA-ANFIS

The ranking results presented in Table 8 reveals that both SE and VC based weighting scheme provided the similar ranking although the ranking values were not identical. Both weighting schemes found the FA-ANFIS model to be the best performer, followed by PSO-ANFIS, BBO-ANFIS, and so on (Table 8). The position of the benchmark GD-LSE-ANFIS was fifth for both weighting schemes. In contrast, the benchmark GD-LSE-ANFIS was found to be the top ranked prediction model followed by FA-ANFIS, PSO-ANFIS, ICA-ANFIS, and so on (Table 8) when GRA-based weighting scheme was used. However, the difference in weight between GD-LSE-ANFIS and FA-ANFIS was almost negligible. Therefore, it can be concluded that FA-ANFIS appeared to be the best prediction model in predicting ET_0 values, at least for this example problem presented in this effort. It can also be observed that the evolutionary-algorithm-tuned ANFIS models, especially FA-ANFIS and PSO-ANFIS performed better than the classical ANFIS model (GD-LSE-ANFIS) for the SE and VC based weighting scheme. On the other hand, it is observed that the weight values of the FA-ANFIS and PSO-ANFIS were

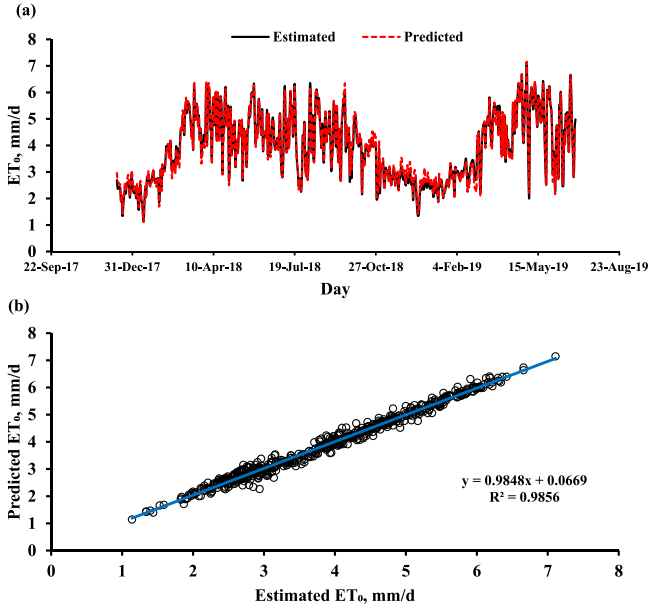

Fig. 8. Prediction accuracy of the developed hybrid FA-ANFIS model over the testing period: (a) FAO-56 PM estimated and model predicted ET_0 time series, (b) scatterplots of the FAO-56 PM estimated versus model predicted ET_0.

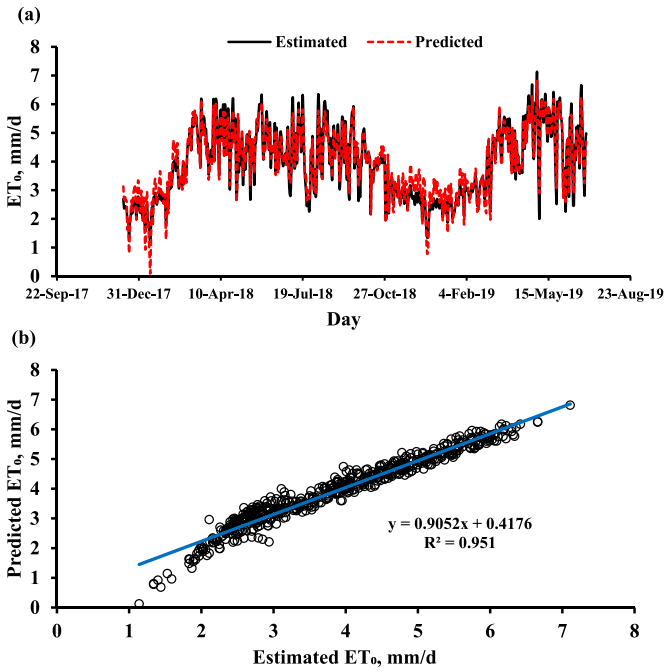

Fig. 9. Prediction accuracy of the developed hybrid ACOR-ANFIS model over the testing period: (a) FAO-56 PM estimated and model predicted ET_0 time series, (b) scatterplots of the FAO-56 PM estimated versus model predicted ET_0.

the same (0.445), and that the top ranked GD-LSE-ANFIS had almost the same weight value (0.447) for the GRA based weighting scheme. Therefore, it can be argued that the FA-ANFIS model achieved a better performance relative to the others as indicated by the ranking scores computed using the three decision theories. The FA-ANFIS is suggested as the best hybrid ANFIS model to predict daily ET_0 values for this study.

To evaluate the models with the help of diagrams besides the tables and to evaluate further the performances of the best (FA-ANFIS) and worst (ACOR-ANFIS) hybrid ANFIS models, model performances were illustrated schematically using scatter and hydrograph plots. Figs. 8–9 display the comparisons of the estimated (FAO-56 PM calculated ET_0) and predicted (hybridized model outputs) daily ET_0 values.

The estimated versus predicted plots (Figs. 8(a) and 9(a)) clearly indicate that FA-ANFIS produced a superior matching between the estimated and predicted daily ET_0 lines (Fig. 8(a)) when compared to the ACOR-ANFIS produced daily ET_0 lines (Fig. 9(a)). The scatter plots displayed in Fig. 8(b) and 9(b) reveal that there was less scatter/dispersion around the fit line for the FA-ANFIS model (Fig. 8(b)) than the ACOR-ANFIS model (Fig. 9(b)). An observation of the hydrograph plots reveals that the peak points of the ET_0 time series were well captured and modelled by the FA-ANFIS model than the ACOR-ANFIS model.

7. Overall findings

This study assessed prediction performances of several optimization algorithm tuned ANFIS models and proposed a raking of these models using three decision theories (SE, VC, and GRA) that incorporated various performance evaluation indices in reaching the conclusion. Therefore, the overall findings consisted of two parts: (a) assessing the prediction performances of the developed models to predict daily ET_0 based on several performance evaluation indices (as described in section "5. Performance evaluation of the developed models"), and (b) providing a ranking of the models through incorporating a set of performance evaluation indices within a framework of decision theories given the fact that standalone prediction models often provide conflicting performances. When considering prediction capabilities of ANFIS models in predicting daily ET_0, as presented in Table 7 and Figs. 7, 8, and 9, some of the major findings are as follows:

(1) The mean and median of the absolute error values between the FAO-56 PM estimated and FA-ANFIS model predicted ET_0 were the minimum (mean = 0.113 mm/d and median = 0.082 mm/d), which indicated the superior performance of the FA-ANFIS model when compared to other models.
(2) In quantitative terms, FA-ANFIS model provided the best results for most of the performance evaluation indices (R = 0.993, NS = 0.986, IOA = 0.996, KGE = 0.989, MAD = 0.054 mm/d, RMSE = 0.149 mm/d, and NRMSE = 3.819%). On the other hand, CA-ANFIS produced the worst prediction accuracies (NS = 0.944, IOA = 0.984, KGE = 0.883, RMSE = 0.294 mm/d, NRMSE = 7.507%, and a10-index = 0.792) when compared with others. The values of these performance evaluation indices clearly indicated the superior and inferior performances, respectively, of the FA-ANFIS and CA-ANFIS models in predicting daily ET_0.
(3) Although FA-ANFIS produced superior performances with respect to most of the performance evaluation indices, three indices (IOA, MAE, and a^{10}-index) suggested the superiority of PSO-ANFIS, TLBO-ANFIS, and GD-LSE-ANFIS, respectively among others.
(4) CA-ANFIS proved to be the worst performer for the six performance evaluation indices (NS, IOA, KGE, RMSE, NRMSE, and a^{10}-index). However, the performance of ACOR-ANFIS was found to be inferior with respect to R and MAD criteria whereas BA-ANFIS showed poor performance when MAD criterion was used.

Based on the obtained results, it can be concluded that the performances of different ANFIS models were ranked differently when different performance evaluation indices were computed based on the models' performance on test dataset. This contradiction in prediction performances was overcome by applying three decision theories to provide a fair ranking of the prediction models. When ranking results are considered, the following conclusions can be drawn:

(1) Both SE and VC weighting schemes found the FA-ANFIS model to be the best performer, followed by PSO-ANFIS, BBO-ANFIS, and so on (Table 8).
(2) When GRA-based weighting scheme was used, the GD-LSE-ANFIS was found to be the top ranked prediction model followed by FA-ANFIS, PSO-ANFIS, ICA-ANFIS, and so on (Table 8). Nevertheless, the difference in weight between GD-LSE-ANFIS and FA-ANFIS was almost negligible. Therefore, it can be concluded that FA-ANFIS appeared to be the best prediction model in predicting ET_0 values, at least for this example problem presented in this effort.

To sum up, the overall findings of the study revealed that the proposed modelling approach was able to provide hundreds even thousands of future ET_0 estimates without the need for calculating point ET_0 values for a particular set of input variables. In other words, future values of ET_0 can be obtained from the developed relationship between the climatic variables and ET_0 (relationship contained in the ANFIS models) rather than computing ET_0 values from the climatic variables using the FAO-56 PM equations. Of note, the basis for developing this input-output relationship is entirely based on ET_0 computations using the FAO-56 PM method.

8. Discussion

Reference evapotranspiration (ET_0) values predicted using the followed methodology in this study were compared to FAO-56 PM estimated ET_0 values during training, validation, and testing phases as presented and discussed earlier in section "6. Results". The ET_0

calculated using FAO-56 PM was regarded as the standard value, and the ET_0 predicted by the proposed optimization algorithm tuned ANFIS models were compared with the standard value. The results of the hybrid ANFIS model which performed best (i.e., FA-ANFIS) were compared with those of the hybrid models presented in previous literature for daily ET_0 prediction. What is more, this study provided a robust decision support tool to select the best AI based prediction models using three decision theories (SE, VC, and GRA). The literature review illustrated that the model selection techniques had been rarely utilized to determine the best prediction model from a choice of several alternatives when predicting daily ET_0. Recently, Roy et al. (2020) used decision theories to calculate weights of standalone hybrid models to be integrated in an ensemble modelling approach for predicting daily ET_0. They employed five evolutionary algorithm tuned AI models compared to 15 evolutionary algorithm tuned hybrid ANFIS models presented and compared in this study.

One of the prime aims of this study was to propose several hybrid ANFIS models developed through coupling ANFIS and optimization algorithms for predicting daily ET_0. The performance comparison between the classical ANFIS (GD-LSE-ANFIS) and optimization algorithm tuned hybrid ANFIS models demonstrated that the hybrid ANFIS models especially FA-ANFIS performed better than the classical ANFIS model to predict the daily ET_0 for the studied station. This finding can be justified since optimization algorithms generally improve ANFIS training phase, which is validated by the validation datasets, and consequently, the trained and validated ANFIS models provide a better result in terms of prediction accuracy. Previous literature on AI based hybrid models further justify superior performances of the optimization approaches for coupling through AI based models (Ahmadi et al., 2021; Mohammadi and Mehdizadeh, 2020; Guan et al., 2020; Mohammadi et al., 2020; Mehdizadeh et al., 2020; Safari et al., 2020).

Deciding on the number of input variables for the AI based modelling techniques including hybridized ANFIS models has been the most crucial phase in developing any prediction tools. Several recent studies on ET_0 modelling employed different variable selection procedures in reaching conclusion about the optimal number of input variables (Ahmadi et al., 2021; Mohammadi and Mehdizadeh, 2020; Tao et al., 2018), which produced the optimal prediction performance. These studies reported that models with all possible climatic variables as inputs generally provided with the best results. Upon conducting several trials on different combinations of input variables, the present study also observed the similar findings, i.e., prediction accuracy of hybrid ANFIS models improved with the number of input variables considered. Therefore, the results presented in this study is based on employing all possible climatic variables (maximum and minimum air temperatures, relative humidity, wind speed, and sunshine hours) as inputs to the developed hybrid ANFIS models.

The superiority of AI based machine learning models over the empirical models in predicting ET_0 values has been well documented in recent literature, especially the hybridized models with optimization algorithms or pre-processing tools (Fan et al., 2020; Wu et al., 2020). However, AI based modelling approaches often suffers from model over- or under-fitting issues that need to be addressed adequately before employing the models for prediction purposes. An over-fitted model usually provides sufficient accuracy during the training phase, however, fails to produce expected accuracy during the validation phase. In other words, the difference between training and validation performances is huge for an over-fitted AI model. These over-fitted AI models are expected to provide higher prediction errors when tested with the unseen test dataset. A careful inspection was performed during the model development phase to make sure that the difference between the training and validation errors are minimal and within the acceptable limits. Therefore, the developed hybridized ANFIS models do not suffer from the model over-fitting issue as the training and validation results were carefully examined during the model development stage.

Recently, optimization algorithms have attained increasing attention as techniques of enhancing ET_0 modelling with AI based approaches (Ahmadi et al., 2021; Chia et al., 2021; Mohammadi and Mehdizadeh, 2020; Tao et al., 2018). The findings of the previous studies confirmed the superiority of optimization algorithm tuned hybrid models in predicting daily or monthly ET_0 values. The results of the best prediction model (FA-ANFIS) in this research were compared with the optimal hybrid ET_0 modelling approaches proposed in previous studies. Although several performance indices were computed on the test dataset to test the performances of the developed hybrid ANFIS models in this study, the available indices computed in previous studies were used for the comparison purpose. The values of performance indices during the testing phase for the best hybrid ANFIS model (FA-ANFIS) are as follows: $R = 0.993$, $R^2 = 0.986$ (obtained from R value of 0.993), NS = 0.986, IOA = 0.996, KGE = 0.989, MAD = 0.054 mm/d, RMSE = 0.149 mm /d, NRMSE = 3.819%, and SI = 0.038 (obtained from NRMSE value of 3.819%).

The findings in this study may not be explicitly comparable to other studies due to differences in study conditions in terms of geographical locations and modelling tools applied. However, the numeric values of different performance evaluation indices were found comparable or even better than those of the recently published papers on ET_0 modelling. For instance, the findings of the present study were better than Tao et al. (2018), who reported that the best hybrid FA-ANFIS achieved SI, R^2 and RMSE values of 0.043, 0.97 and 0.24 mm/d, respectively, for the prediction of ET_0 at a site in Bur Dedougou, Burkina Faso. The FA-ANFIS developed in this study also produced superior performance than the SVR-IWD model proposed in Ahmadi et al. (2021), reported that the optimal SVR-IWD models achieved the following performances at various stations: at the Arak station (RMSE = 0.404 mm/d, R = 0.980), at Mashhad station (RMSE = 0.540 mm/d, R = 0.983), at the Shiraz station (RMSE = 0.299 mm/d, R = 0.989), at the Bandar Abbas station (RMSE = 0.457 mm/d, R = 0.962), at the Tehran station (RMSE = 0.55 9 mm/d, R = 0.978), at the Yazd station (RMSE = 0.399 mm/d, R = 0.986). In addition, the findings obtained in the present study are in line with the findings presented in Chia et al. (2021), who found that the best ELM-WOA produced an average RMSE and R^2 values of 0.0011–0.1972 mm/d and 1.0000–0.9486 for the considered three stations. Our results also obtained higher and comparable performances, respectively in terms of RMSE and R^2 criteria presented in Mohammadi and Mehdizadeh (2020), who obtained RMSE and R^2 values for the RF-SVR-WOA model as follows: RMSE = 0.213 mm/d and $R^2 = 0.991$ at Isfahan station; RMSE = 0.325 mm/d and $R^2 = 0.977$ at Urmia station; RMSE = 0.257 mm/d and $R^2 = 0.991$ at Yazd station.

To assess the prediction accuracies of various optimization algorithm tuned ANFIS models in predicting ET_0, nine statistical performance evaluation indices were used in this study. Most of the studies reported in recent literature used few of these performance indices in determining the performance of ET_0 prediction models. It is apparent that the performances of different prediction models produce different ranking when these indices are employed to test the model's performance during the testing phase (Roy et al., 2020). This nature of the prediction models demands the incorporation of several performance indices within the framework of suitable decision tools in determining the suitability of a standalone prediction model compared to others. Therefore, to address this contradictory behavior of the developed models, the present study divided the performance indices into benefit (the higher the better) and cost (the lower the better) indices to be used in the framework of decision theories for providing a more reliable ranking of the developed prediction models. These analyses revealed that three decision theories (SE, VC, and GRA) used in this study introduced different ranking values to predict daily ET_0 values and that the FA-ANFIS and ACOR-ANFIS were the best and worst prediction models, respectively. The literature review illustrated that this model selection technique utilizing decision theories had been rarely used to provide a ranking of the ET_0 prediction models. Recently, Roy et al. (2020) employed decision theories to rank optimization algorithm tuned ANFIS models (five optimization

algorithms were used). The present study utilized 15 optimization algorithms to enhance the performance of ANFIS models and provided a comprehensive comparison among the hybrid models with the aid of three decision theories, which provided rankings of the developed hybrid models. The proposed ranking approaches provided a robust decision support tool that would facilitate the decision makers in the right choice of the best prediction model in determining daily ET_0 for the considered study area.

Overall, the present study provides the following outcomes, which are highly significant in the field of ET_0 forecasting using AI based modelling techniques. First, this study demonstrated a method for developing hybridized ANFIS models that do not suffer from the model over-fitting. This was done through careful observation of the training and validation results. Second, the performance of the trained and validated models was tested using a new unseen test dataset (used neither for training nor for validation). The test results, which was verified by comparing the results with other similar studies found in the literature, also demonstrated the suitability of the proposed hybrid ANFIS models especially FA-ANFIS in predicting daily ET_0. Therefore, this model (FA-ANFIS) could be easily used in large-scale applications for efficient water management. Lastly, this study provides a relatively new method for best predictive model selection technique utilizing decision theories. This has huge application potential in the field of agriculture, engineering, and water management.

In sum, this study is of significant benefit as it provides a solution to a critical agricultural problem. The methods employed in this study provides an accurate and robust ET_0 prediction tool, which can provide the foundation for designing effective irrigation scheduling schemes and help in resourceful management of water uses in agriculture. Also, the developed hybrid prediction tool can be applied universally provided relevant datasets are available.

9. Conclusions

In this study, 15 evolutionary algorithms, i.e., Artificial Bee Colony (ABC), Bee Algorithm (BA), Biogeography-based Optimization (BBO), Continuous Ant Colony Optimization (ACOR), Covariance Matrix Adaptation Evolution Strategy (CMA-ES), Cultural Algorithm (CA), Differential Evolution (DE), Firefly Algorithm (FA), Genetic Algorithm (GA), Harmony Search (HS), Imperialist Competitive Algorithm (ICA), Invasive Weed Optimization (IWO), Particle Swarm Optimization (PSO), Simulated Annealing (SA) and Teaching-Learning-based Optimization (TLBO) were used to develop hybridized ANFIS models for ET_0 forecasting. The performances of these hybridized ANFIS models were compared with those of the classic ANFIS model (GD-LSE-ANFIS). The methodology was demonstrated using a case study in a sub-tropical climate in Bangladesh. It was observed that performance evaluation indices utilized in this study did not favor a single hybridized model. For example, the performance evaluation results suggested that FA-ANFIS was evidenced to be the best prediction model among the 16 individual models for most of the performance evaluation indices, except the IOA, MAE, and a^{10}-index for which PSO-ANFIS, TLBO-ANFIS, and GD-LSE-ANFIS showed the superior performance. On the other hand, CA-ANFIS proved to be the worst performer for the six performance evaluation indices (NS, IOA, KGE, RMSE, NRMSE, and a^{10}-index). Decision making in such situations is quite challenging and selecting a single hybridized model is a difficult task. To resolve this issue, Shannon's Entropy, VC, and GRA based decision theories that takes into account several performance indices instead of relying on a single index were applied to select the best preforming model. This study concluded that FA-ANFIS was the best prediction model in predicting ET_0 values, at least for this example problem utilized. Overall, this study provides an accurate and early ET_0 prediction tool, which can provide the foundation for designing effective irrigation scheduling schemes and help in resourceful management of water uses in agriculture.

Funding

This research did not receive any specific grant from funding agencies in the public, commercial, or not-for-profit sectors.

Declaration of Competing Interest

The authors declare that they have no known competing financial interests or personal relationships that could have appeared to influence the work reported in this paper.

Data Availability

Datasets are available with the authors and will be available on request.

Acknowledgements

The authors appreciate the use of the open-source MATLAB code "YPEA: Yarpiz Evolutionary Algorithms" [https://yarpiz.com/477/ypea-yarpiz-evolutionary-algorithms] written by the Yarpiz team.

References

Ahmadi, F., Mehdizadeh, S., Mohammadi, B., Pham, Q.B., DOAN, T.N.C., Vo, N.D., 2021. Application of an artificial intelligence technique enhanced with intelligent water drops for monthly reference evapotranspiration estimation. Agric. Water Manag. 244, 106622 https://doi.org/10.1016/j.agwat.2020.106622.

Allen, R.G., Pereira, L.S., Raes, D., Smith, M., 1998. Crop evapotranspiration—guidelines for computing crop water requirements, FAO Irrig. Drain. Pap. No. 56, Rome.

Allen, R.G., Pereira, L.S., Raes, D., 2006. Evapotranspiración del cultivo. Guías para la determinación de los requerimientos de agua de los cultivos (Technical report). FAO, Roma, Itália.

Allen, R.G., Pereira, L.S., Howell, T.A., Jensen, M.E., 2011. Evapotranspiration information reporting: I. Factors governing measurement accuracy. Agric. Water Manag. 98, 899–920. https://doi.org/10.1016/j.agwat.2010.12.015.

Atashpaz-Gargari, E., Lucas, C., 2007. Imperialist competitive algorithm: an algorithm for optimization inspired by imperialistic competition, in: Proceedings of the 2007 IEEE Congress on Evolutionary Computation. pp. 4661–4667. ⟨https://doi.org/10.1109/CEC.2007.4425083⟩.

Azad, A., Manoochehri, M., Kashi, H., Farzin, S., Karami, H., Nourani, V., Shiri, J., 2019. Comparative evaluation of intelligent algorithms to improve adaptive neuro-fuzzy inference system performance in precipitation modelling. J. Hydrol. 571, 214–224. https://doi.org/10.1016/j.jhydrol.2019.01.062.

Bezdek, J.C., Ehrlich, R., Full, W., 1984. FCM: the fuzzy c-means clustering algorithm. Comput. Geosci. 10, 191–203. https://doi.org/10.1016/0098-3004(84)90020-7.

Cerny, V., 1985. Thermodynamical approach to the traveling salesman problem: an efficient simulation algorithm. J. Optim. Theory Appl. 45, 41–51.

Chen, P., 2019. On the diversity-based weighting method for risk assessment and decision-making about natural hazards. Entropy 21, 1–13. https://doi.org/10.3390/e21030269.

Chia, M.Y., Huang, Y.F., Koo, C.H., 2021. Swarm-based optimization as stochastic training strategy for estimation of reference evapotranspiration using extreme learning machine. Agric. Water Manag. 243, 106447 https://doi.org/10.1016/j.agwat.2020.106447.

Citakoglu, H., Cobaner, M., Haktanir, T., Kisi, O., 2014. Estimation of monthly mean reference evapotranspiration in Turkey. Water Resour. Manag. 28, 99–113. https://doi.org/10.1007/s11269-013-0474-1.

Cobaner, M., 2011. Evapotranspiration estimation by two different neuro-fuzzy inference systems. J. Hydrol. 398, 292–302. https://doi.org/10.1016/j.jhydrol.2010.12.030.

Dang, V.-H., Vien, N.A., Chung, T., 2019. A covariance matrix adaptation evolution strategy in reproducing kernel Hilbert space. Genet. Program. Evol. Mach. 20, 479–501. https://doi.org/10.1007/s10710-019-09357-1.

Das, S., Suganthan, P.N., 2011. Differential evolution: a survey of the state-of-the-art. IEEE Trans. Evol. Comput. 15, 4–31. https://doi.org/10.1109/TEVC.2010.2059031.

Deb, K., Pratap, A., Agarwal, S., Meyarivan, T., 2002. A fast and elitist multiobjective genetic algorithm: NSGA-II. IEEE Trans. Evol. Comput. 6, 182–197. https://doi.org/10.1109/4235.996017.

Deng, J.-L., 1982. Control problems of grey systems. Syst. Control Lett. 1, 288–294. https://doi.org/10.1016/S0167-6911(82)80025-X.

Ding, L., Shao, Z., Zhang, H., Xu, C., Wu, D., 2016. A comprehensive evaluation of urban sustainable development in China based on the TOPSIS-entropy method. Sustainability 8, 746.

Dorigo, M., 1992. Optimization, Learning and Natural Algorithms. Politecnico di Milano, Italy (in Italian).

Dorigo, M., Maniezzo, V., Colorni, A., 1996. Ant system: optimization by a colony of cooperating agents. IEEE Trans. Syst. Man Cybern. Part B 26, 29–41. https://doi.org/10.1109/3477.484436.

Dorigo, M., Caro, G.D., Gambardella, L.M., 1999. Ant algorithms for discrete optimization. Artif. Life 5, 137–172. https://doi.org/10.1162/106454699568728.
Du, D., Simon, D., Ergezer, M., 2009. Biogeography-based optimization combined with evolutionary strategy and immigration refusal, in: Proceedings of the 2009 IEEE International Conference on Systems, Man and Cybernetics. pp. 997–1002. ⟨https://doi.org/10.1109/ICSMC.2009.5346055⟩.
Elbeltagi, A., Deng, J., Wang, K., Malik, A., Maroufpoor, S., 2020. Modeling long-term dynamics of crop evapotranspiration using deep learning in a semi-arid environment. Agric. Water Manag. 241, 106334 https://doi.org/10.1016/j.agwat.2020.106334.
Fan, H.-Y., Lampinen, J., 2003. A trigonometric mutation operation to differential evolution. J. Glob. Optim. 27, 105–129. https://doi.org/10.1023/A:1024653025686.
Fan, J., Wu, L., Ma, X., Zhou, H., Zhang, F., 2020. Hybrid support vector machines with heuristic algorithms for prediction of daily diffuse solar radiation in air-polluted regions. Renew. Energy 145, 2034–2045. https://doi.org/10.1016/j.renene.2019.07.104.
Fang, G., Guo, Y., Huang, X., Rutten, M., Yuan, Y., 2018. Combining Grey relational analysis and a bayesian model averaging method to derive monthly optimal operating rules for a hydropower reservoir. Water 10, 1–20.
Fatemeh, K., Lee, T.S., Thamer, A.M., Mohammadreza, A., Najmeh, K., 2012. Daily evapotranspiration modeling from limited weather data by using neuro-fuzzy computing technique. J. Irrig. Drain. Eng. 138, 21–34. https://doi.org/10.1061/(ASCE)IR.1943-4774.0000343.
Feng, Y., Cui, N., Gong, D., Zhang, Q., Zhao, L., 2017a. Evaluation of random forests and generalized regression neural networks for daily reference evapotranspiration modelling. Agric. Water Manag. 193, 163–173. https://doi.org/10.1016/j.agwat.2017.08.003.
Feng, Y., Jia, Y., Cui, N., Zhao, L., Li, C., Gong, D., 2017b. Calibration of Hargreaves model for reference evapotranspiration estimation in Sichuan basin of southwest China. Agric. Water Manag. 181, 1–9. https://doi.org/10.1016/j.agwat.2016.11.010.
Feng, Y., Peng, Y., Cui, N., Gong, D., Zhang, K., 2017c. Modeling reference evapotranspiration using extreme learning machine and generalized regression neural network only with temperature data. Comput. Electron. Agric. 136, 71–78. https://doi.org/10.1016/j.compag.2017.01.027.
Ferreira, L.B., da Cunha, F.F., de Oliveira, R.A., Fernandes Filho, E.I., 2019. Estimation of reference evapotranspiration in Brazil with limited meteorological data using ANN and SVM – a new approach. J. Hydrol. 572, 556–570. https://doi.org/10.1016/j.jhydrol.2019.03.028.
Gao, X.Z., Govindasamy, V., Xu, H., Wang, X., Zenger, K., 2015. Harmony search method: Theory and applications. Comput. Intell. Neurosci. 2015, 1–10. https://doi.org/10.1155/2015/258491.
Geem, Z.W., Kim, J., Loganathan, G.V., 2001. A new heuristic optimization algorithm: harmony search. Simulation 76, 60–68. https://doi.org/10.1177/003754970107600201.
Geman, S., Geman, D., 1984. Stochastic relaxation, Gibbs distributions, and the bayesian restoration of images. IEEE Trans. Pattern Anal. Mach. Intell. PAMI- 6, 721–741. https://doi.org/10.1109/TPAMI.1984.4767596.
Goldberg, D.E., 1989. Genetic Algorithms in Search, Optimization and Machine Learning, 1st ed. Addison-Wesley Longman Publishing Co., Inc., USA.
Goyal, M.K., Bharti, B., Quilty, J., Adamowski, J., Pandey, A., 2014. Modeling of daily pan evaporation in sub tropical climates using ANN, LS-SVR, Fuzzy Logic, and ANFIS. Expert Syst. Appl. 41, 5267–5276. https://doi.org/10.1016/j.eswa.2014.02.047.
Granata, F., 2019. Evapotranspiration evaluation models based on machine learning algorithms—a comparative study. Agric. Water Manag. 217, 303–315. https://doi.org/10.1016/j.agwat.2019.03.015.
Guan, Y., Mohammadi, B., Pham, Q.B., Adarsh, S., Balkhair, K.S., Rahman, K.U., Linh, N.T.T., Tri, D.Q., 2020. A novel approach for predicting daily pan evaporation in the coastal regions of Iran using support vector regression coupled with krill herd algorithm model. Theor. Appl. Climatol. 142, 349–367. https://doi.org/10.1007/s00704-020-03283-4.
Hansen, N., Müller, S.D., Koumoutsakos, P., 2003. Reducing the time complexity of the derandomized evolution strategy with covariance matrix adaptation (CMA-ES). Evol. Comput. 11, 1–18. https://doi.org/10.1162/106365603321828970.
Hassanvand, M.R., Karami, H., Mousavi, S.-F., 2018. Investigation of neural network and fuzzy inference neural network and their optimization using meta-algorithms in river flood routing. Nat. Hazards 94, 1057–1080. https://doi.org/10.1007/s11069-018-3456-z.
Ingber, L., 1989. Very fast simulated re-annealing. Math. Comput. Model. 12, 967–973. https://doi.org/10.1016/0895-7177(89)90202-1.
Ingber, L., 1996. Adaptive simulated annealing (ASA): Lessons learned. Control Cyber 25, 33–54.
Jang, J.-S.R., 1993. ANFIS: adaptive-network-based fuzzy inference system. IEEE Trans. Syst. Man Cybern. 23, 665–685. https://doi.org/10.1109/21.256541.
Jang, J.-S.R., Sun, C.T., Mizutani, E., 1997. Neuro-Fuzzy and Soft Computing: A Computational Approach to Learning and Machine Intelligence. Prentice Hall, Upper Saddle River, New Jersey.
Karaboga, D., 2005. An idea based on honey bee swarm for numerical optimization. Tech. Rep. TR06, ErciyesUniversity, Eng. Fac. Comput. Eng. Dep.
Kennedy, J., Eberhart, R., 1995. Particle swarm optimization, in: Proceedings of ICNN'95 - International Conference on Neural Networks. pp. 1942–1948, vol.4. ⟨https://doi.org/10.1109/ICNN.1995.488968⟩.
Kirkpatrick, S., Gelatt, C.D., Vecchi, M.P., 1983. Optimization by simulated annealing. Science 220 (80), 671–680. https://doi.org/10.1126/science.220.4598.671 (LP).
Kisi, O., Sanikhani, H., Zounemat-Kermani, M., Niazi, F., 2015. Long-term monthly evapotranspiration modeling by several data-driven methods without climatic data. Comput. Electron. Agric. 115, 66–77. https://doi.org/10.1016/j.compag.2015.04.015.
Kumar, M., Raghuwanshi, N.S., Singh, R., 2011. Artificial neural networks approach in evapotranspiration modeling: a review. Irrig. Sci. 29, 11–25. https://doi.org/10.1007/s00271-010-0230-8.
Kuo, H.C., Lin, C.H., 2013. Cultural evolution algorithm for global optimizations and its applications. J. Appl. Res. Technol. 11, 510–522. https://doi.org/10.1016/S1665-6423(13)71558-X.
Ladlani, I., Houichi, L., Djemili, L., Heddam, S., Belouz, K., 2014. Estimation of daily reference evapotranspiration (ET0) in the north of Algeria using adaptive neuro-fuzzy inference system (ANFIS) and multiple linear regression (MLR) models: a comparative study. Arab. J. Sci. Eng. 39, 5959–5969. https://doi.org/10.1007/s13369-014-1151-2.
Landeras, G., Ortiz-Barredo, A., López, J.J., 2008. Comparison of artificial neural network models and empirical and semi-empirical equations for daily reference evapotranspiration estimation in the Basque Country (Northern Spain). Agric. Water Manag. 95, 553–565. https://doi.org/10.1016/j.agwat.2007.12.011.
Li, Q., Meng, X.X., Liu, Y.B., Pang, L.F., 2019. Risk assessment of floor water inrush using entropy weight and variation coefficient model. Geotech. Geol. Eng. 37, 1493–1501. https://doi.org/10.1007/s10706-018-0702-9.
Li, X., Wang, K., Liu, L., Xin, J., Yang, H., Gao, C., 2011. Application of the entropy weight and TOPSIS method in safety evaluation of coal mines. Procedia Eng. 26, 2085–2091. https://doi.org/10.1016/j.proeng.2011.11.2410.
Liu, W., Li, Q., Zhao, J., 2018. Application on floor water inrush evaluation based on AHP variation coefficient method with GIS. Geotech. Geol. Eng. 36, 2799–2808. https://doi.org/10.1007/s10706-018-0502-2.
López-Urrea, R., de Santa Olalla, Martín, Fabeiro, F., Moratalla, A, C., 2006. Testing evapotranspiration equations using lysimeter observations in a semiarid climate. Agric. Water Manag. 85, 15–26. https://doi.org/10.1016/j.agwat.2006.03.014.
Luo, X., Wang, Y., Zhao, J., Chen, Y., Mo, S., Gong, Y., 2016. Grey relational analysis of an integrated cascade utilization system of geothermal water. Int. J. Green Energy 13, 14–27. https://doi.org/10.1080/15435075.2014.896259.
Mathworks, 2020. Technical documentation [WWW Document], How Genet. algorithm Work. URL ⟨https://au.mathworks.com/help/gads/how-the-genetic-algorithm-works.html⟩ (Accessed 4.10.20).
Mehdizadeh, S., Mohammadi, B., Bao Pham, Q., Nguyen Khoi, D., Thi Thuy Linh, N., 2020. Implementing novel hybrid models to improve indirect measurement of the daily soil temperature: elman neural network coupled with gravitational search algorithm and ant colony optimization. Measurement 165, 108127. https://doi.org/10.1016/j.measurement.2020.108127.
Mehrabian, A.R., Lucas, C., 2006. A novel numerical optimization algorithm inspired from weed colonization. Ecol. Inform. 1, 355–366. https://doi.org/10.1016/j.ecoinf.2006.07.003.
Metropolis, N., Rosenbluth, A.W., Rosenbluth, M.N., Teller, A.H., Teller, E., 1953. Equation of state calculations by fast computing machines. J. Chem. Phys. 21, 1087–1092. https://doi.org/10.1063/1.1699114.
Mohammadi, B., Mehdizadeh, S., 2020. Modeling daily reference evapotranspiration via a novel approach based on support vector regression coupled with whale optimization algorithm. Agric. Water Manag. 237, 106145 https://doi.org/10.1016/j.agwat.2020.106145.
Mohammadi, B., Ahmadi, F., Mehdizadeh, S., Guan, Y., Pham, Q.B., Linh, N.T.T., Tri, D. Q., 2020. Developing novel robust models to improve the accuracy of daily streamflow modeling. Water Resour. Manag. 34, 3387–3409. https://doi.org/10.1007/s11269-020-02619-z.
Patil, A.P., Deka, P.C., 2017. Performance evaluation of hybrid Wavelet-ANN and Wavelet-ANFIS models for estimating evapotranspiration in arid regions of India. Neural Comput. Appl. 28, 275–285. https://doi.org/10.1007/s00521-015-2055-0.
Peyghami, M.R., Khanduzi, R., 2013. Novel MLP neural network with hybrid Tabu search algorithm. Neural Netw. World 23, 255–270.
Pham, D.T., Ghanbarzadeh, A., Koç, E., Otri, S., Rahim, S., Zaidi, M., 2006. The Bees Algorithm — A Novel Tool for Complex Optimisation Problems. In: Pham, D.T., Eldukhri, E.E., Soroka, A.J.B.T.-I.P.M., S. (Eds.). Elsevier Science Ltd, Oxford, pp. 454–459. https://doi.org/10.1016/B978-008045157-2/50081-X.
Pincus, M., 1970. Letter to the Editor—a Monte Carlo method for the approximate solution of certain types of constrained optimization problems. Oper. Res. 18, 1225–1228. https://doi.org/10.1287/opre.18.6.1225.
Price, K.V., 1999. An introduction to differential evolution. In: Corne, D., Dorigo, M., Glover, F. (Eds.), New Ideas in Optimization. McGraw-Hill Ltd, UK, GBR, pp. 79–108.
Rao, R.V., Savsani, V.J., Vakharia, D.P., 2011. Teaching–learning-based optimization: a novel method for constrained mechanical design optimization problems. Comput. Des. 43, 303–315. https://doi.org/10.1016/j.cad.2010.12.015.
Reynolds, R., 1994. An introduction to cultural algorithms.
Roy, D.K., Datta, B., 2018. Selection of meta-models to predict saltwater intrusion in coastal aquifers using entropy weight based decision theory, in: Proceedings of the 2018 IEEE Conference on Technologies for Sustainability (SusTech). pp. 1–6. ⟨https://doi.org/10.1109/SusTech.2018.8671371⟩.
Roy, D.K., Datta, B., 2019. Adaptive management of coastal aquifers using entropy-set pair analysis–based three-dimensional sequential monitoring network design. J. Hydrol. Eng. 24, 04018072 https://doi.org/10.1061/(ASCE)HE.1943-5584.0001765.
Roy, D.K., Barzegar, R., Quilty, J., Adamowski, J., 2020. Using ensembles of adaptive neuro-fuzzy inference system and optimization algorithms to predict reference

evapotranspiration in subtropical climatic zones. J. Hydrol. 591, 125509 https://doi.org/10.1016/j.jhydrol.2020.125509.
Safari, M.J.S., Mohammadi, B., Kargar, K., 2020. Invasive weed optimization-based adaptive neuro-fuzzy inference system hybrid model for sediment transport with a bed deposit. J. Clean. Prod. 276, 124267 https://doi.org/10.1016/j.jclepro.2020.124267.
Sanikhani, H., Deo, R.C., Samui, P., Kisi, O., Mert, C., Mirabbasi, R., Gavili, S., Yaseen, Z. M., 2018. Survey of different data-intelligent modeling strategies for forecasting air temperature using geographic information as model predictors. Comput. Electron. Agric. 152, 242–260. https://doi.org/10.1016/j.compag.2018.07.008.
Shannon, C.E., 1948. A mathematical theory of communication. Bell Syst. Tech. J. 27, 379–423. https://doi.org/10.1002/j.1538-7305.1948.tb01338.x.
Shiri, J., Nazemi, A.H., Sadraddini, A.A., Landeras, G., Kisi, O., Fakheri Fard, A., Marti, P., 2014. Comparison of heuristic and empirical approaches for estimating reference evapotranspiration from limited inputs in Iran. Comput. Electron. Agric. 108, 230–241. https://doi.org/10.1016/j.compag.2014.08.007.
Simon, D., 2008. Biogeography-based optimization. IEEE Trans. Evol. Comput. 12, 702–713. https://doi.org/10.1109/TEVC.2008.919004.
Socha, K., Dorigo, M., 2008. Ant colony optimization for continuous domains. Eur. J. Oper. Res. 185, 1155–1173. https://doi.org/10.1016/j.ejor.2006.06.046.
Song, Y., Liu, M., Wang, Z., 2010. Biogeography-based optimization for the traveling salesman problems, in: Proceedings of the 2010 Third International Joint Conference on Computational Science and Optimization. pp. 295–299. ⟨https://doi.org/10.1109/CSO.2010.79⟩.
Storn, R., 1999. Designing digital filters with differential evolution. In: Corne, D., Dorigo, M., Glover, F. (Eds.), New Ideas in Optimization. McGraw-Hill Ltd, UK, GBR, pp. 109–126.
Storn, R., Price, K., 1997. Differential evolution – a simple and efficient heuristic for global optimization over continuous spaces. J. Glob. Optim. 11, 341–359. https://doi.org/10.1023/A:1008202821328.
Sugeno, M., Yasukawa, T., 1993. A fuzzy-logic-based approach to qualitative modeling. IEEE Trans. Fuzzy Syst. 1, 7. https://doi.org/10.1109/TFUZZ.1993.390281.
Sun, L., Song, X., Chen, T., 2019. An improved convergence particle swarm optimization algorithm with random sampling of control parameters. J. Control Sci. Eng. 72, 7478498 https://doi.org/10.1155/2019/7478498.
Szu, H., Hartley, R., 1987. Fast simulated annealing. Phys. Lett. A 122, 157–162. https://doi.org/10.1016/0375-9601(87)90796-1.
Takagi, T., Sugeno, M., 1985. Fuzzy identification of systems and its applications to modeling and control. IEEE Trans. Syst. Man Cybern. SMC- 15, 116–132. https://doi.org/10.1109/TSMC.1985.6313399.
Tao, H., Diop, L., Bodian, A., Djaman, K., Ndiaye, P.M., Yaseen, Z.M., 2018. Reference evapotranspiration prediction using hybridized fuzzy model with firefly algorithm: regional case study in Burkina Faso. Agric. Water Manag. 208, 140–151. https://doi.org/10.1016/j.agwat.2018.06.018.
van Laarhoven, P.J.M., Ohki, Y., Teferra, D., 2020. Simulated annealing: theory and applications.
Wang, S., Lian, J., Peng, Y., Hu, B., Chen, H., 2019. Generalized reference evapotranspiration models with limited climatic data based on random forest and gene expression programming in Guangxi, China. Agric. Water Manag. 221, 220–230. https://doi.org/10.1016/j.agwat.2019.03.027.
Wang, T., Chen, J.-S., Wang, T., Wang, S., 2015. Entropy weight-set pair analysis based on tracer techniques for dam leakage investigation. Nat. Hazards 76, 747–767. https://doi.org/10.1007/s11069-014-1515-7.
Wang, Z., Rangaiah, G.P., 2017. Application and analysis of methods for selecting an optimal solution from the Pareto-optimal front obtained by multiobjective optimization. Ind. Eng. Chem. Res. 56, 560–574. https://doi.org/10.1021/acs.iecr.6b03453.
Werbos, P.J., 1974. Beyond Regression: New Tools for Prediction and Analysis in the Behavioral Sciences. Harvard University.
Wu, J., Sun, J., Liang, L., Zha, Y., 2011. Determination of weights for ultimate cross efficiency using Shannon entropy. Expert Syst. Appl. 38, 5162–5165. https://doi.org/10.1016/j.eswa.2010.10.046.
Wu, L., Zhou, H., Ma, X., Fan, J., Zhang, F., 2019. Daily reference evapotranspiration prediction based on hybridized extreme learning machine model with bio-inspired optimization algorithms: application in contrasting climates of China. J. Hydrol. 577, 123960 https://doi.org/10.1016/j.jhydrol.2019.123960.
Wu, L., Huang, G., Fan, J., Ma, X., Zhou, H., Zeng, W., 2020. Hybrid extreme learning machine with meta-heuristic algorithms for monthly pan evaporation prediction. Comput. Electron. Agric. 168, 105115 https://doi.org/10.1016/j.compag.2019.105115.
Wu, L., Peng, Y., Fan, J., Wang, Y., Huang, G., 2021. A novel kernel extreme learning machine model coupled with K-means clustering and firefly algorithm for estimating monthly reference evapotranspiration in parallel computation. Agric. Water Manag. 245, 106624 https://doi.org/10.1016/j.agwat.2020.106624.
Xiang, K., Li, Y., Horton, R., Feng, H., 2020. Similarity and difference of potential evapotranspiration and reference crop evapotranspiration – a review. Agric. Water Manag. 232, 106043 https://doi.org/10.1016/j.jhydrol.2004.10.024.
Xu, H., Ma, C., Lian, J., Xu, K., Chaima, E., 2018. Urban flooding risk assessment based on an integrated k-means cluster algorithm and improved entropy weight method in the region of Haikou, China. J. Hydrol. 563, 975–986. https://doi.org/10.1016/j.jhydrol.2018.06.060.
Xu, Q., Xu, K., 2018. Mine safety assessment using gray relational analysis and bow tie model. PLoS One 13, 0193576. https://doi.org/10.1371/journal.pone.0193576.
Yan, S., Wu, L., Fan, J., Zhang, F., Zou, Y., Wu, Y., 2021. A novel hybrid WOA-XGB model for estimating daily reference evapotranspiration using local and external meteorological data: applications in arid and humid regions of China. Agric. Water Manag. 244, 106594 https://doi.org/10.1016/j.agwat.2020.106594.
Yang, X.-S., 2009. Harmony search as a metaheuristic algorithm. In: Geem, Z.W. (Ed.), Music-inspired harmony search algorithm: Theory and applications. Springer Berlin Heidelberg, Berlin, Heidelberg, pp. 1–14. https://doi.org/10.1007/978-3-642-00185-7_1.
Yang, X.-S., 2010. Firefly algorithm, stochastic test functions and design optimisation. Int. J. Bio Inspir. Comput. 2. https://doi.org/10.1504/IJBIC.2010.032124.
Yu, H., Wen, X., Li, B., Yang, Z., Wu, M., Ma, Y., 2020. Uncertainty analysis of artificial intelligence modeling daily reference evapotranspiration in the northwest end of China. Comput. Electron. Agric. 176, 105653 https://doi.org/10.1016/j.compag.2020.105653.
Yuce, B., Packianather, M.S., Mastrocinque, E., Pham, D.T., Lambiase, A., 2013. Honey bees inspired optimization method: the bees algorithm. Insects 4, 646–662. https://doi.org/10.3390/insects4040646.
Zhang, L., Xie, X., 2010. Application of identical degree of set pair analysis on software refactoring, in: Proceedings of the 2010 International Conference on Computational Intelligence and Software Engineering. pp. 1–4. ⟨https://doi.org/10.1109/CISE.2010.5676831⟩.
Zhang, Z., Qiao, P., Qi, Q., Xu, J., Li, Y., Zheng, Z., 2010. Study on the multi-factor degree set pair analysis fuzzy evaluation model based on entropy weight, in: Proceedings of the 2010 3rd International Conference on Biomedical Engineering and Informatics. pp. 2979–2984. ⟨https://doi.org/10.1109/BMEI.2010.5639338⟩.
Zheng, Y., Ling, J., Wu, H.-F., Xue, J.-Y, X.-B., 2014. Localized biogeography-based optimization. Soft Comput. 18, 2323–2334. https://doi.org/10.1007/s00500-013-1209-1.
Zotarelli, L., Dukes, M.D., Romero, C.C., Migliaccio, K.W., Kelly, T., 2010. Step by step calculation of the Penman-Monteith Evapotranspiration (FAO-56 method), Technical document number: AE459, Agricultural and Biological Engineering Department, UF/ IFAS Extension, USDA.